Eur. Phys. J. A (2025) 61:260
https://doi.org/10.1140/epja/s10050-025-01741-z

THE EUROPEAN PHYSICAL JOURNAL A

Review

Neutron Poisons and neutron sources - from the nuclear point of view

Michael Wiescher[1,a], **Richard James deBoer**[1,b], **Joachim Görres**[1], **Lothar Buchmann**[2], **Chris Ruiz**[2]

[1] Department of Physics and Astronomy, University of Notre Dame, Notre Dame, IN 46556, USA
[2] TRIUMF, Vancouver, BC V6T 2A3, Canada

Received: 22 August 2025 / Accepted: 2 November 2025

Communicated by Maria Borge

Abstract This paper is in memory of Roberto Gallino, a long-time collaborator on questions of neutron sources and neutron-induced reactions in stellar nucleosynthesis. We therefore discuss a topic that was of great interest to him, the correlation between neutron sources that provide the neutron flux for the production of heavy elements in the *s*-process and neutron poison reactions that reduce the number of neutrons in the stellar environment. Neutron poisons play a role in all *s*-process environments, such as the final phase of core helium burning of massive stars or the carbon pocket in hydrogen-helium intershell environment of low-mass AGB stars, originally proposed by Gallino and his co-workers more than 40 years ago. This paper will argue that neutron poison reactions serve as a neutron storage mechanism through which neutron sources can be fueled to provide a delayed neutron release.

1 Introduction

Neutron capture reactions on highly abundant light nuclei such as carbon, nitrogen, oxygen, and neon are considered to be neutron poisons that reduce the overall neutron flux in stellar environments. It was Roberto Gallino who pointed out many times that the neutrons absorbed in these reactions will eventually be released, contributing as neutron sources to the neutron-induced nucleosynthesis pattern in a delayed manner [1]. Yet, no detailed analysis exists of the associated reaction flow that determines the correlation between the neutron poison and the eventual neutron release processes. A reaction network, triggered by neutron capture reactions on light nuclei, depends on the possible subsequent reactions, the overall abundances of neutrons and α-particles and the strength of the associated reaction processes in helium burning environments. This paper is primarily focused on investigating the strength of the associated neutron absorption and neutron production processes.

It should be pointed out that the expression "neutron poison" is somewhat misleading; while the abundance of carbon, nitrogen, oxygen, and other light nuclei are frequently orders of magnitude higher than the abundances of those above the iron peak, the radiative neutron capture cross sections on light nuclei are typically in the micro-barn range at helium burning energies, low compared to cross sections in the milli-barn to barn range for more massive nuclei. The low-energy cross sections of neutron capture reactions are typically – with a few exceptions – described by the $1/v$-law for *s*-wave neutron capture ($\ell = 0$) in which the amplitude of the cross sections is determined primarily by the contributions from direct capture and subthreshold resonances. The $1/v$ law for *s*-waves translates into a dependence on $1/\sqrt{E}$ (since $v = (2E/\mu)^{1/2}$) and the reaction rate $\langle \sigma v \rangle_{X(n,\gamma)}$ for neutron capture on an isotope X can be expressed in terms of the Maxwellian averaged cross section (MACS) [2]. The MACS show variations from a constant value at low temperatures and towards higher values at higher temperature due to non-resonant contributions with higher orbital momenta and potentially resonant contributions [3]. In some cases, such as in the $^{14}C(n,\gamma)^{15}C$ reaction, the low-energy cross section for neutron capture is determined by *p*-wave capture ($\ell = 1$) and the low-energy cross section declines with energy $\sigma \propto v$ [4,5].

The level density in light compound nuclei is naturally much lower than in the case of heavy nuclei, which explains the small cross sections for light nuclei by the largely reduced resonance contributions. Since the effective depletion of neutrons in a stellar burning environment depends on the abundances of the capturing isotopes as well as the neutron capture rates, the depletion of neutrons can be summarized by

[a] e-mail: mwiesche@nd.edu (corresponding author)
[b] e-mail: Richard.J.deBoer.12@nd.edu

Published online: 17 November 2025

the following equation:

$$\frac{dY_n}{dt} = -Y_n \cdot \lambda_n - \sum_x Y_x \cdot Y_n \cdot \rho \cdot \langle \sigma v \rangle_{X(n,\gamma)} - \sum_p Y_p \cdot Y_n \cdot \rho \cdot \left(\langle \sigma v \rangle_{P(n,\gamma)} + \langle \sigma v \rangle_{P(n,p)} + \langle \sigma v \rangle_{P(n,\alpha)} \right)$$

with Y_n representing the average neutron abundance and ρ the density of stellar matter; λ_n is the natural decay constant for the β^- decay of the neutron and $\langle \sigma v \rangle$ are the temperature dependent reaction rates for the different reactions absorbing neutrons. Y_X represent the abundances of the nuclei at higher masses – typically with $Z \geq 26$ and Y_P stands for highly abundant light nuclei that can act as neutron poisons, decaying through the γ-, p-, and α-channel. Taking into account typical abundances and reaction cross sections, roughly 50% of the neutrons are absorbed by neutron poison nuclei P while the rest may be available for the build-up of heavier elements in an s-process, i-process, or even an n-process environment, as recently discussed and summarized [6].

In addition to neutron poisons, neutron sources will influence the neutron budget in a stellar burning environment. Neutron sources are, in most cases, helium-induced exothermic (α, n) reactions with positive Q-values and reaction rates that increase exponentially with temperature due to the tunneling probability through the Coulomb barrier. In addition, there may be endothermic (α, n) reactions with negative Q-values, which only activate above a certain temperature threshold. Proton-induced (p, n) reactions are endothermic, requiring temperatures well above those expected for stellar core burning. Deuteron- and triton-induced reactions may contribute to neutron production in the case of sufficient abundance for these isotopes. For conditions such as those anticipated for Big Bang nucleosynthesis [7], neutron production reactions might be ^{3}H$(d, n)^4$He, as well as ^{6,7}Li$(d, n)^{7,8}$Be, which would help to maintain the neutron flux. These could also be complemented by triton-induced reactions such as ^{3}He$(t, n)^5$Li, ^{6,7}Li$(t, n)^{8,9}$Be, as well as ^{7}Be$(t, n)^9$B possibly followed by the ^{9}Be$(t, n)^{11}$B and ^{9}B$(t, n)^{11}$C reactions [8–10].

For this paper, we limit ourselves to the α-particle-induced neutron sources because of the typically low abundances of the heavy hydrogen isotopes in quiescent [11] and explosive stellar environments [12]. The neutron production at any such site can then be expressed in terms of the very temperature-sensitive correlated reaction rates $\langle \sigma v \rangle_{(\alpha,n)}$:

$$\frac{dY_n}{dt} = +\sum_x Y_s \cdot Y_\alpha \cdot \rho \cdot \langle \sigma v \rangle_{S(\alpha,n)}$$

with Y_S the abundance of the respective source isotopes and $S(\alpha, n)$ the specific neutron sources that could be triggered. For additional neutron sources, the corresponding reaction terms would need to be added. The efficiency of these α-induced neutron sources in releasing neutrons depends on the associated reaction rates, which, unlike most of the neutron capture processes, are very dependent on the temperature of the helium-burning environment. Because of the rapidly declining cross section with energy, the reaction probability for charged particle reactions is traditionally presented in terms of the S-factor $S(E)$, which corresponds to the cross section $\sigma(E)$ with the $\ell = 0$ penetrability of tunneling through the Coulomb barrier approximately removed, where its dependence on the de Broglie wavelength is reflected by the energy term in the equation:

$$S(E) = E\,\sigma(E)\,e^{2\pi\eta}. \tag{1}$$

The reaction rate is expressed as

$$N_A \langle \sigma v \rangle_{S(\alpha,n)} = N_A \left(\frac{8}{\pi \mu_{tA}} \right)^{1/2} \frac{1}{(kT)^{3/2}} \int_0^\infty S(E) \exp\left[-\frac{E}{kT} - 2\pi\eta \right] dE.$$

The parameter η approximates the impact of the Coulomb barrier and is defined as $\eta = (\mu_{tA}/2E)^{1/2} e^2 Z_t Z_A/\hbar$ with μ_{tA} as the reduced mass of the reaction system in atomic mass units and N_A being Avogadro's number.

2 *s*-process sites

The s-process takes place during a number of helium burning conditions in stars and relies on the α-particle induced production of neutrons. Therefore, the efficiency for neutron production depends sensitively on the temperature and density conditions at the s-process site as well as on the abundance of the seed isotopes for neutron production. The two sites we discuss here are the one responsible for the weak s-process associated with core helium burning in massive stars [13] and the site of the main s-process linked to the carbon pocket in the hydrogen-helium inter-shell region of low mass asymptotic giant branch (AGB) stars [14,15].

Several of the evaluated neutron- and α-capture data presented in this work are based on calculations using the multi-channel, multi-level R-matrix code AZURE2 [16], which provides a method to uniquely highlight the close correspondence between the two reaction channels through a comprehensive analysis of the respective compound systems. In depth details of the calculations are not given as they are meant to illustrate the general characteristics of the cross sections and the links between different reaction types. Comprehensive evaluations of each reaction are beyond the scope of the current work.

2.1 Neutron poisons and sources in core helium burning of massive stars

Core helium burning in massive stars has been identified as the most likely site for the weak s-process. The neutron production is based on the preexisting abundance of ^{14}N as the most abundant CNO isotope generated during the preceding hydrogen burning phase. With the onset of helium burning after the core contraction phase of a red giant star, the existing ^{14}N is rapidly converted through a sequence of α-capture reactions, starting with the ^{14}N$(\alpha,\gamma)^{18}$F reaction [17] followed by the β-decay of ^{18}F and the subsequent ^{18}O$(\alpha,\gamma)^{22}$Ne reaction [18–20], which feeds the ^{22}Ne$(\alpha,n)^{25}$Mg neutron source. Although the first two α-capture reactions are fast, the actual ^{22}Ne$(\alpha,n)^{25}$Mg neutron source [21–27] is delayed due to its negative Q-value. It is only gradually activated during the contraction phase of the helium core toward the very end of helium burning as higher temperatures are reached [28,29].

At this point, the mass fraction of the contracting helium burning core of the star is increasingly converted to ^{12}C and ^{16}O via the 3α-process [30] and the subsequent ^{12}C$(\alpha,\gamma)^{16}$O reaction [31], respectively. Despite the low cross section, a fair fraction of the neutrons released will be captured via the ^{12}C$(n,\gamma)^{13}$C(n,γ) reactions feeding the long-lived ^{14}C isotope. A similar neutron poison sequence is initiated by neutron capture via the ^{16}O$(n,\gamma)^{17}$O reaction with the reaction product converted primarily by a subsequent neutron capture, the ^{17}O(n,α) reaction, to again produce ^{14}C. The efficiency of these two processes for neutron absorption needs to be investigated. The long-lived ^{14}C ($T_{1/2} = 5730y$) is depleted by p-wave neutron capture [5,32] to ^{15}C or, at sufficiently high temperatures, may undergo α-capture via the ^{14}C$(\alpha,\gamma)^{18}$O [33] and ^{18}O$(\alpha,\gamma)^{22}$Ne reactions, feeding back into the ^{22}Ne$(\alpha,n)^{25}$Mg neutron source. In this case, neutron capture on ^{12}C [34] and ^{16}O [35], as well as on ^{22}Ne [36] may impact the neutron budget.

While during the release period neutrons are primarily captured on ^{12}C [34] and ^{16}O [35], additional neutron capture can occur on the neutron seed nucleus ^{22}Ne via the ^{22}Ne$(n,\gamma)^{23}$Ne reaction [36]. This occurs primarily at lower temperatures, prior to the onset of the ^{22}Ne$(\alpha,n)^{25}$Mg reaction. Once temperatures have increased sufficiently to activate the ^{22}Ne$(\alpha,n)^{25}$Mg reaction, additional neutron capture can occur via the ^{25}Mg$(n,\gamma)^{26}$Mg reaction [37–39], demonstrating a close correlation between the neutron source and neutron poisons. Experiments have shown that in addition to the latter neutron capture reaction, another α-induced neutron source, the ^{25}Mg$(\alpha,n)^{28}$Si reaction, may emerge [40]. However, while the source will be largely reduced as a result of the increasing Coulomb barrier, it may play a stronger role under the higher temperature conditions achieved during the carbon-burning phase in massive stars.

2.2 Neutron poisons and sources in the carbon pocket of low mass AGB stars

A case of special interest is the model of the carbon pocket in the hydrogen-helium inter-shell region, which has been identified as the neutron source for the main s-process [14,41–43]. In its present interpretation, hydrogen is mixed with a mass fraction of up to $X_H \leq 5\times10^{-4}$ in the inter-shell range and is subsequently and completely captured by ^{12}C via the ^{12}C$(p,\gamma)^{13}$N reaction with the latter decaying to ^{13}C. It is argued that the limit on the hydrogen mass fraction ensures that all mixed hydrogen is captured by existing ^{12}C to eventually form ^{13}C without triggering subsequent proton capture reactions forming a complete CNO cycle, because this would lead to the production of neutron poison reactions such as ^{13}C$(n,\gamma)^{14}$C and ^{14}N$(n,p)^{14}$C. This s-process model and its parameters are typically tested against the observed s-process abundance distribution within the framework of different parameter assumptions for the carbon pocket [44].

The typical temperature in the carbon pocket during the long-term quiescent period is around 0.1 GK, but it gradually increases through a bottom heating process that triggers a short convective phase during which temperatures can increase to a level at which the ^{22}Ne$(\alpha,n)^{25}$Mg neutron source can be initiated. This would require ^{14}N as seed material; it has been suggested that this will be mixed from the helium burning shell into the inter-shell range. Within the chosen parameter space [6,42,45–49], the model appears to be able to provide a neutron flux sufficient to reproduce the observed s-process abundance distribution, which is interpreted as a basis for the success of the model.

However, all of these studies are based on the assumption of limited hydrogen inflow, so that all of the protons can be successfully absorbed to form ^{13}C without any subsequent proton capture such as the ^{13}C$(p,\gamma)^{14}$N reaction feeding the strong ^{14}N$(n,p)^{14}$C neutron poison reaction [50]. This assumption fails to take into account that nuclear reaction processes are parallel and not sequential processes. This is well-known for the CNO cycle, in which, depending on the temperature, an equilibrium between the different participating isotopes is quickly established. This equilibrium does not depend on the abundance of hydrogen as shown in Wiescher et al. [51]. This suggests that the production of neutron poisons can be expected to be a coherent part of the neutron source and needs to be considered in the framework of a full reaction network for the conditions and through the evolution of the carbon pocket in thermally pulsing AGB stars.

3 The reaction patterns of neutron sources and poisons

In both of the scenarios discussed above, the main neutron poisons are the neutron capture reactions on the more

abundant CNO nuclei. The $^{12}C(n,\gamma)^{13}C$ and the subsequent $^{13}C(n,\gamma)^{14}C$ reactions are considered to be strong neutron absorbers as recently evaluated [52], while the neutron capture on ^{14}C decreases towards lower energies because it is dominated by a p-wave capture component [4,5].

In addition to neutron capture on carbon, the $^{16}O(n,\gamma)^{17}O$ reaction, with multiple direct capture and resonant transitions, has been identified as a strong neutron absorber [35] that could influence the time scale and efficiency of the s-process [53]. This reaction is followed by the $^{17}O(n,\alpha)^{14}C$ reaction, converting the ^{17}O towards lower masses as discussed earlier [54]. The combination of these reactions represents the most dominant neutron absorption process in the carbon-oxygen enriched environment during the final phase of core helium burning. These reactions may also play an important role in the carbon pocket if the CNO equilibrium is established. In that case, an additional neutron poison reaction would be $^{14}N(n,p)^{14}C$, which again would cause the production of long-lived ^{14}C in the carbon pocket. Figure 1 shows a comparison of the neutron capture cross section of the three carbon isotopes ^{12}C, ^{13}C and ^{14}C, based on an R-matrix analysis of the available experimental data.

For the $^{12}C(n,\gamma)^{13}C$ reaction, the s-wave capture is a result of direct radiative capture, resonant capture into the E_x = 3.09 MeV subthreshold state and direct capture into the third excited state (E_x = 3.68 MeV). The R-matrix fit presented here uses external (or channel) capture to model the radiative capture process, which is the standard method implemented in the AZURE2 code [16] and has been used previously by Mughabghab et al. [61] to model both the $^{12}C(n,\gamma)^{13}C$ and $^{13}C(n,\gamma)^{14}C$ reactions. A significant contribution to the ground state transition cross sections comes from the subthreshold resonance at E_x = 3.09 MeV (Γ_{γ_0} = 0.464(42) eV [62], ANC_n = 1.84(16) $fm^{-1/2}$ [63]). The radiative capture data were fit simultaneously with the $^{12}C(n,\text{total})$ data of Auchampaugh et al. [64] (similar to Hale and Paris [65]), which also independently constrained the neutron ANCs of the bound states. For the $^{13}C(n,\gamma)^{14}C$ and $^{14}C(n,\gamma)^{15}C$ reactions, the low energy behavior results primarily from direct radiative capture to the ground state via s and p-wave, respectively. While only the total radiative capture cross sections are shown in Fig. 1, the R-matrix fits were performed using the cross sections for the partial γ-ray transitions.

At helium burning temperatures, the reaction rates are largely determined by the cross section at higher energies, above ≈10 keV. For the $^{12}C(n,\gamma)^{13}C$ reaction, the cross section becomes dominated by p-wave direct radiative capture through the first excited state, as shown by the partial cross section measurements of Nagai et al. [55] and Ohsaki et al. [56]. The situation is similar for the $^{13}C(n,\gamma)^{14}C$ reaction, as observed by Shima et al. [58] and Wallner et al. [59]. In addition to the capture via p-wave to the first excited state, a resonance contributes strongly to the cross section at E_n = 152(1) keV. The neutron partial width is Γ_n = 3.7(7) keV, but measurements of the γ width vary substantially [66,67], with the most recent being 215^{+84}_{-35} meV [67]. Finally, the cross section predictions for the $^{14}C(n,\gamma)^{15}C$ reaction rely largely on the data of Reifarth et al. [60], although a resonance enhancement has been suggested at higher energy (E_n = 1.885 MeV) by Wiescher et al. [4]. More detailed experimental studies are necessary to confirm these data [68] since enrichment in ^{13}C as well as enrichment in ^{14}C will open reaction branches for α-induced break-out from the nCNO cycle as discussed later in this section.

The $^{14}N(n,p)^{14}C$ reaction, which, as a charge exchange process has the highest neutron capture reaction rate in this mass range, is shown in Fig. 8, is expected to be a strong neutron poison associated with neutron production in the carbon pocket. The experimental study of this reaction has been a challenge since the early experimental efforts [69]. Recent accelerator mass spectrometry (AMS) experiments have suggested a decrease in the reaction cross section owing to a deeper interference minimum between the s-wave subthreshold state contribution to the cross section and the low energy tails of higher energy resonances [59]. The corresponding energy range of the $^{14}N(n,p)^{14}C$ reaction was recently mapped again by direct reaction studies at the n_ToF facility at CERN [50]. The results suffer from limited time-of-flight resolution at higher energies as a result of path length and scattering effects, but report good agreement with the AMS measurements when their resolution effects are accounted for. However, these recent studies do not consider previously measured time reverse $^{14}C(p,n)^{14}N$ measurements [70–72], which show different energy dependence over this low energy range. This motivates a more comprehensive comparison of past experimental data and new measurements to resolve these inconsistencies. Figure 2 shows an R-matrix analysis of the $^{14}N(n,p)^{14}C$ reaction that also simultaneously includes all other reaction channels populated through the compound nucleus ^{15}N. While a reasonably good description of a subset of data was obtained, the uncertainty remains significant due to inconsistencies in the cross section found between different data sets.

It should be noted that all of these neutron poison reaction sequences end in the long-lived isotope ^{14}C ($T_{1/2}$ = 5730 y). At low temperatures, the p wave-dominated cross section of $^{14}C(n,\gamma)^{15}C$ reaction is small compared to the neutron capture processes that feed ^{14}C. This causes an enhancement in this isotope, similar to the ^{14}N enhancement in the regular CNO cycle in massive hydrogen-burning stars. At higher temperatures, as expected for helium burning conditions, the neutron capture cross sections on all carbon isotopes are comparable. ^{14}C will be slowly converted to ^{15}C followed by

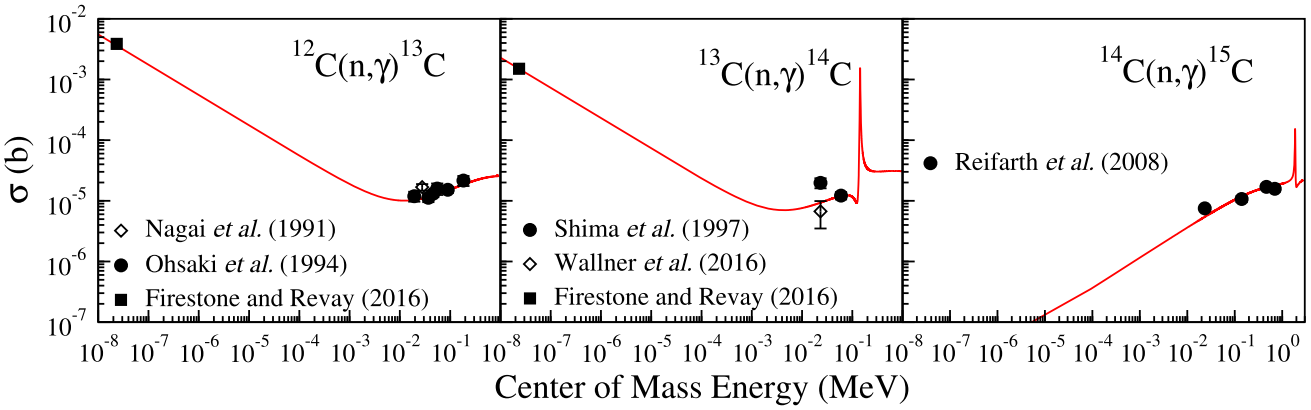

Fig. 1 Reaction cross sections for radiative neutron capture on ^{12}C [55–57], ^{13}C [57–59] and ^{14}C [60]. While the cross sections on ^{12}C and ^{13}C follow the $1/v$ law at low energies, towards higher energies resonance contributions can cause significant enhancement. For the ^{14}C(n,γ) reaction, the cross section is proportional to the velocity but resonance contributions cause further enhancement at higher energies

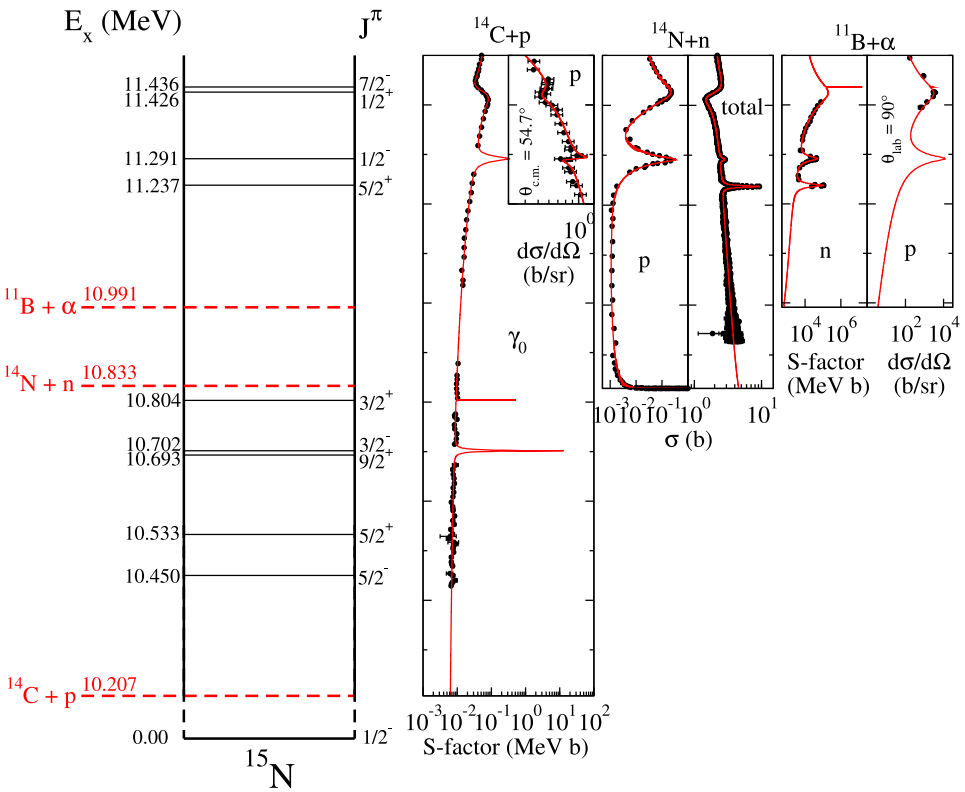

Fig. 2 A level diagram of the ^{15}N system near the proton, neutron and α-particle separation energies compared to a multi-channel R-matrix analysis of the data [70,72–77] over the energy range relevant for the ^{14}N$(n,p)^{14}$C neutron poison reaction rate

β^- decay, feeding ^{15}N$(n,\gamma)^{16}$N [78] with ^{16}N being converted by a second β^- decay back to ^{16}O. Besides the feeding through neutron capture on ^{12}C and ^{14}N, this process resembles a cycle in which four neutrons are converted to ^{4}He by a sequence of four neutron capture reactions interspersed by two β^- decays. In this spirit, the neutron absorption process by CNO nuclei has been labeled as a neutron-driven CNO or nCNO cycle [79] in which the slowest reaction determines the cycle period. The reaction sequence cycle is shown in Fig. 3. It is within such a process that neutrons can be stored until released by sufficiently high cross section α-capture reactions, such as ^{13}C$(\alpha,n)^{16}$O, facilitate a break-out from the cycle feeding neutron source reactions.

4 Neutron induced break-out reactions and a light *s*-process

The closure of the nCNO cycle is facilitated through neutron-induced α-emission via the ^{17}O$(n,\alpha)^{14}$C reaction. Figure 4 shows the R-matrix fit of the cross section based on a recent

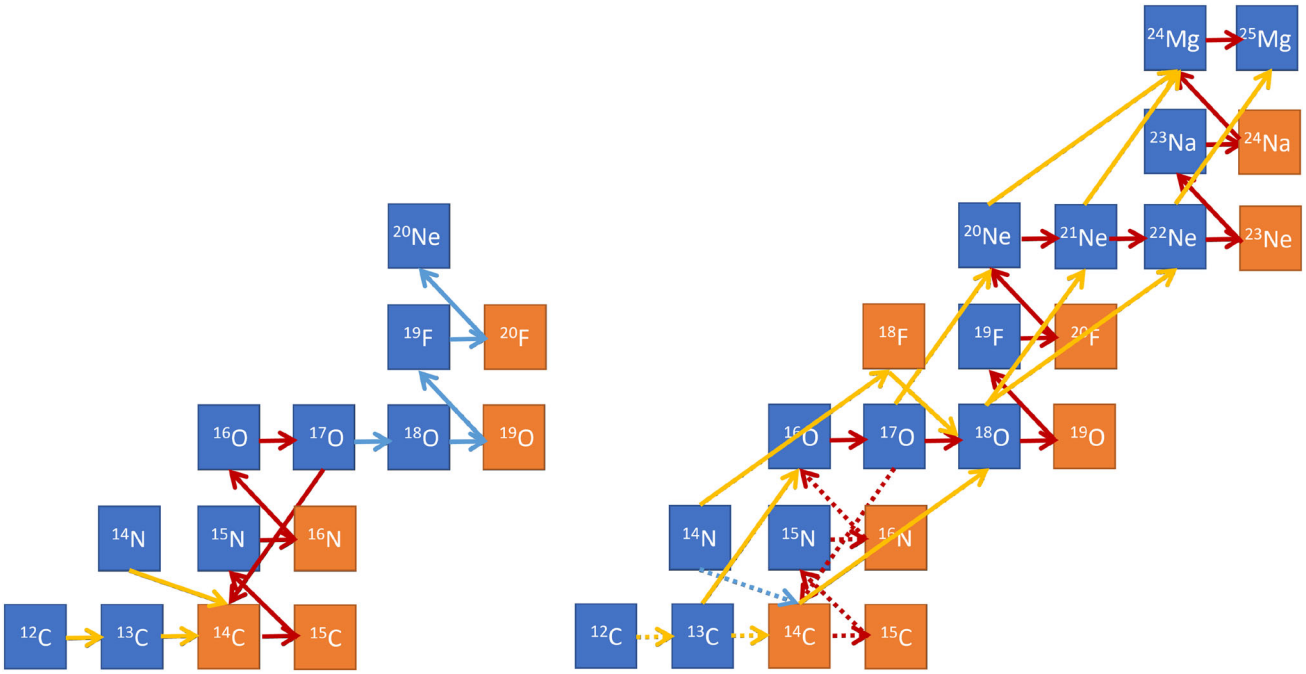

Fig. 3 The left hand side of the figure shows the neutron induced CNO cycle (nCNO) marked in red, which is closed by the $^{17}O(n,\alpha)^{14}C$ reaction. The cycle is fed by neutron capture reactions on ^{12}C, ^{13}C, and ^{14}N marked in yellow. Possible break-out by neutron induced reactions on ^{17}O, ^{18}O, and ^{19}F are marked in blue. For a modest neutron flux, with neutron capture probabilities smaller than the lifetime of the short-lived radioactive isotopes and depending on the strength of the various neutron- or α-induced break-out reactions, the cycle is expected to be closed. The right hand side shows the flow pattern expected for higher temperature conditions. A number of break-out reactions may occur depending on the strength of the radiative neutron capture reactions and exponentially increasing α-capture reactions. The nCNO cycle is marked by dashed red lines, the neutron driven break-out initiating a light s-process by solid red arrows and the α capture driven reaction path by yellow marked arrows

analysis [80,81] that also includes the inverse $^{14}C(\alpha,n)^{17}O$ [82,83], $^{14}C(\alpha,\alpha)^{14}C$ [84,85] and β-delayed α-decay of ^{18}N data [86]. The thermal $^{17}O(n,\alpha)^{14}C$ cross section is up to three orders of magnitude larger [80,87–89] than that of the competing radiative capture process $^{17}O(n,\gamma)^{18}O$ [90]. This ratio is also maintained towards higher energies as suggested by theoretical simulations [91].

As suggested in Fig. 5, at low temperatures, about 1% of the material leaks with each cycle period from the nCNO cycle towards higher masses; even a weaker (n,γ) branch towards higher temperatures establishes a small leak of about 0.3% from the cycle feeding higher Z nuclei via a light s-process like the reaction sequence $^{18}O(n,\gamma)^{19}O(\beta^-\nu)^{19}F(n,\gamma)^{20}F(\beta^-\nu)^{20}Ne$ [92,93] into the Ne-Na mass range as indicated in Fig. 3. Neutron capture reactions by neon isotopes ^{20}Ne, ^{21}Ne and ^{22}Ne [94], with subsequent β-decay to ^{23}Na, link the light s-process pattern via the reaction sequence $^{23}Na(n,\gamma)^{24}Na(\beta^-\nu)^{24}Mg$ that decays into the magnesium-aluminum range. The $^{23}Na(n,\gamma)^{24}Na$ reaction has been experimentally studied and found to be weaker than previously anticipated [95]. This could cause an increase in ^{23}Na and influence the feeding of the magnesium chain. In this case, the two magnesium isotopes $^{25,26}Mg$ become the most important neutron poisons due to their strong neutron capture cross sections, in the milli-barn range [37,38]. This is comparable to the strength of the neutron capture on ^{56}Fe, which is typically considered to be the starting point of s-process nucleosynthesis, feeding the heavier elements. The efficiency of neutron capture reactions within the light s-process chain therefore determines the efficiency of neutron poisons through neutron absorption and the reduction of neutron flux for the s-process, feeding the higher mass abundance distribution.

5 α-induced breakout reactions and neutron sources

Parallel to the light s-process, other break-out reactions are triggered by α-capture reactions. This mirrors the break-out from the hot CNO cycle at high temperatures as discussed in Wiescher et al. [79], which occurs via the $^{14}O(\alpha,p)^{17}F(p,\gamma)^{18}Ne(\alpha,p)^{21}Na$ or alternatively via the $^{15}O(\alpha,\gamma)^{19}Ne(p,\gamma)^{20}Ne$ chain and depends on the reaction rates for the α capture. The break-out from the nCNO cycle is facilitated by the two α-capture reactions releasing neutrons with $^{13}C(\alpha,n)^{16}O$ and $^{17}O(\alpha,n)^{20}Ne$ being

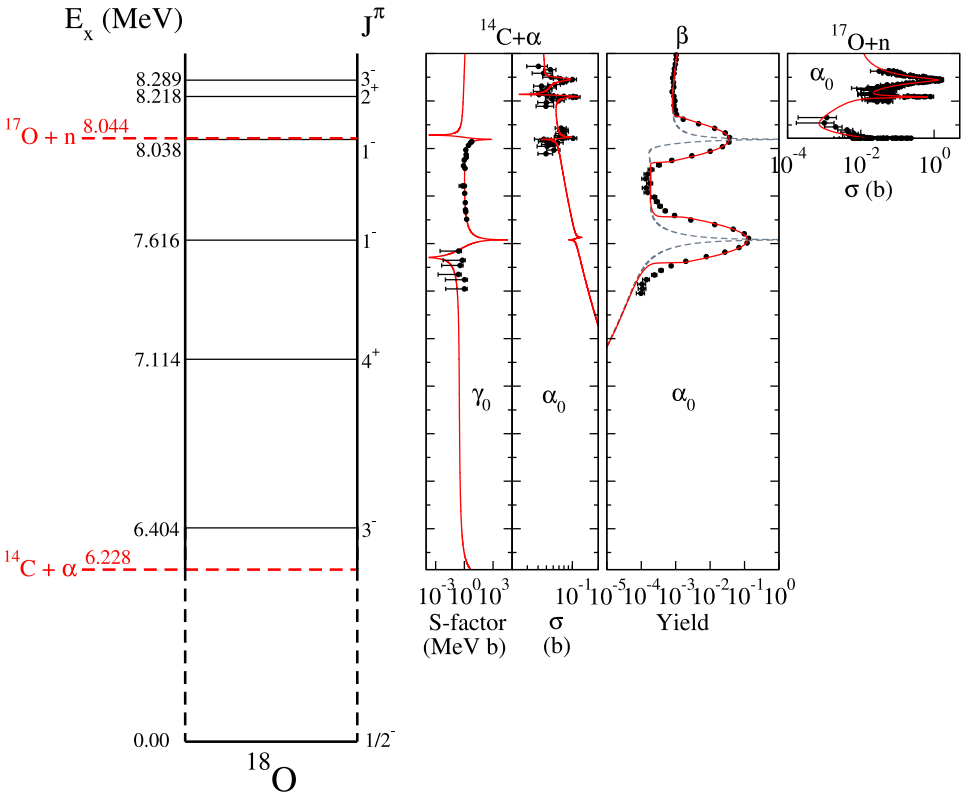

Fig. 4 The level scheme of ^{18}O and the associated cross sections of the $^{17}O(n,\alpha)^{14}C$ reaction based on a recent analysis of the existing reaction data Guardo et al. [80,81], cross section data of the inverse $^{14}C(\alpha,n)^{17}O$ reaction [82,83] and the $^{14}C(\alpha,\gamma)^{17}O$ reaction [33], $^{14}C(\alpha,\alpha)^{14}C$ scattering [84,85], as well as the analysis of the β-delayed α-decay of ^{18}N through the 1^- states in ^{18}O [86]. The gray dashed lines in the $^{18}N(\beta\alpha)^{14}C$ plot indicate the bare R-matrix calculation, while the red solid line is with the experimental resolution applied

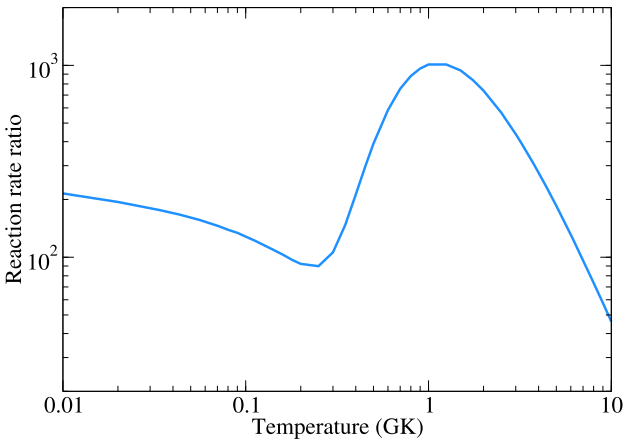

Fig. 5 The ratio of the reaction rates for the $^{17}O(n,\alpha)^{14}C$ over the $^{17}O(n,\gamma)^{18}O$ radiative capture reactions based on the rates given by Oliva et al. [81] and Zhang et al. [91], respectively. Typically the strong interaction based (n,α) reaction process is up to three orders of magnitude stronger than the electromagnetic interaction based radiative capture. The ratio declines towards lower temperature suggesting a roughly 1% loss of material from the cycle per period towards higher masses. The period or cycle time is determined by the slowest neutron capture or decay rates within the cycle

the most dominant. In addition, there are chains of radiative α-capture reactions leading to neutron source reactions at higher masses. The first one is direct via the $^{14}C(\alpha,\gamma)^{18}O(\alpha,\gamma)^{22}Ne(\alpha,n)^{25}Mg(\alpha,n)^{28}Si$ chain, while the second chain is impeded by the β^+ decay of ^{18}F, $^{14}N(\alpha,\gamma)^{18}F(\beta^-\nu)^{18}O(\alpha,\gamma)^{22}Ne$, again followed by neutron release via $^{22}Ne(\alpha,n)^{25}Mg(\alpha,n)^{28}Si$. This means that the α-capture reactions eventually lead to release of neutrons, causing the reaction path to move toward the $N = Z$ line. The efficiency of these neutron production reactions depends on the aforementioned reaction rates for the respective α capture processes. While the branchings between neutron and α capture processes depend on the respective rates, they depend more so on the abundance of ^{4}He fuel and neutron flux in the burning environment. In the following, we will summarize the conditions for the most important sites for α-induced neutron production processes in quiescent stellar helium burning environments.

The $^{13}C(\alpha,n)^{16}O$ reaction has been studied over a wide energy range, most notably in deep underground experiments at the LUNA [96] and JUNA [97] facilities, even mapping into the high energy portion of the Gamow range of the reaction. Detailed R-matrix analysis of the available reaction data associated with the compound nucleus ^{17}O indicate a more reliable determination of the cross section over a wide energy range due largely to the improved consistency between the different measurements and reduced uncertainties. In the low-energy range, the cross section is characterized by the impact of a pronounced near-threshold state, which causes an enhancement in the corresponding S-factor [98].

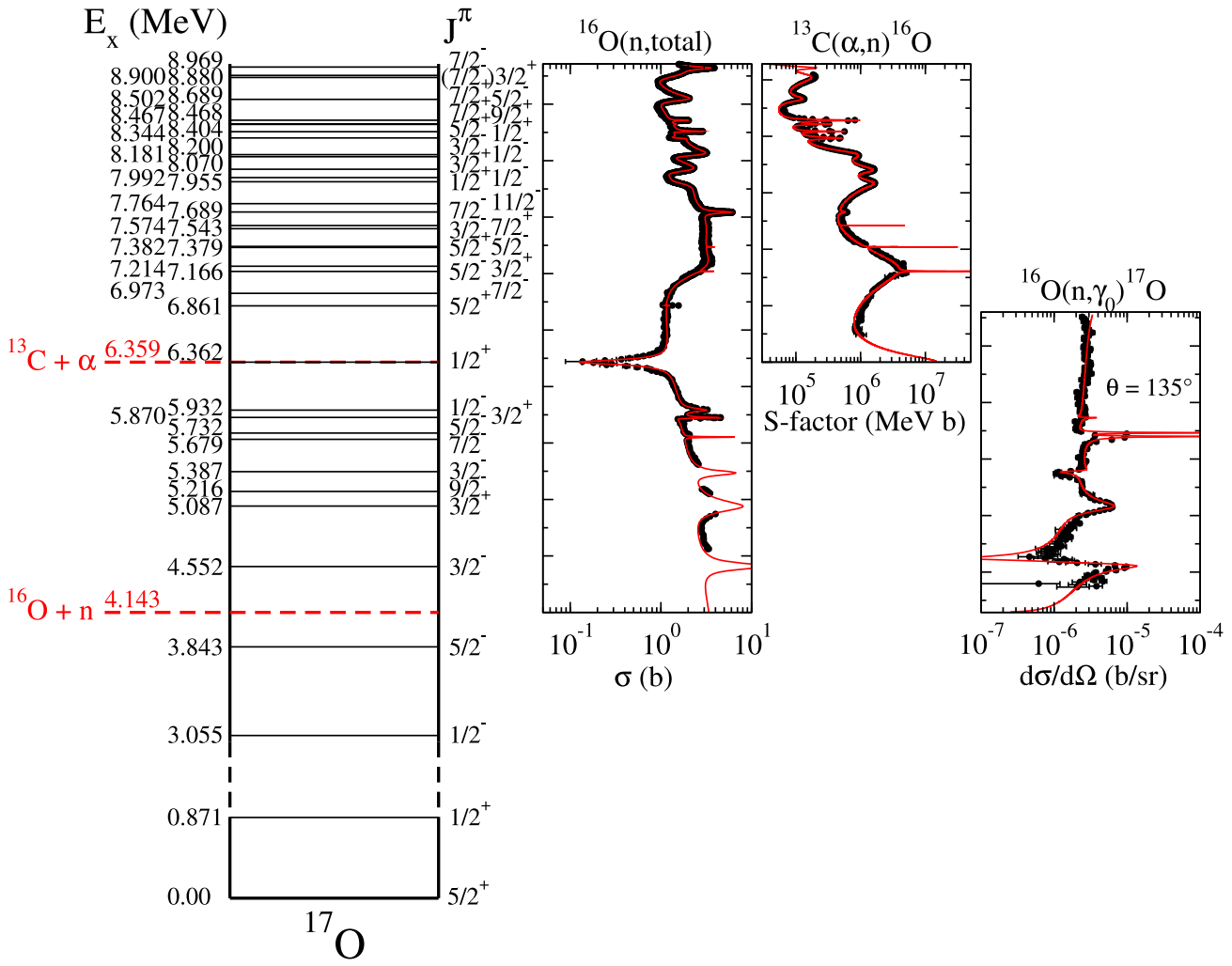

Fig. 6 Level diagram of the ^{17}O system near neutron and α-particle separation energies compared with an R-matrix fit to the ^{16}O+n total neutron cross section data of Fowler et al. [103] and Cierjacks et al. [104], the ^{13}C$(\alpha, n)^{16}$O data of Bair and Haas [105] and Gao et al. [97] and the ^{16}O$(n, \gamma_0)^{17}$O data of Holt et al. [102]

Figure 6 shows the level scheme of the compound nucleus ^{17}O, and the associated R-matrix fit of the data, demonstrating how the different levels near and above the α-threshold determine the S-factor over an energy range of ≈2.5 MeV, which corresponds to the typical temperature range of stellar helium burning. The ^{13}C$(\alpha, n)^{16}$O reaction is followed by the ^{16}O$(n, \gamma)^{17}$O neutron absorber reaction [35]. The cross section data [99–101] of this reaction and the time-inverse ^{17}O$(\gamma, n)^{16}$O [102] are well reproduced in the R-matrix fit and correspond closely to the known level structure in the ^{17}O compound nucleus above the neutron threshold. The subsequent ^{17}O$(n, \alpha)^{14}$C reaction leads to the production of ^{14}C as outlined earlier. With increasing temperature, the α-capture reaction ^{14}C$(\alpha, \gamma)^{18}$O leads to the production of ^{18}O, opening new reaction channels such as ^{18}O$(n, \gamma)^{19}$O$(\beta^-)^{19}$F and ^{18}O$(\alpha, \gamma)^{22}$Ne.

There is limited information on the reaction cross section for ^{14}C$(\alpha, \gamma)^{18}$O; at low energies, several resonances near the threshold have been predicted to contribute to the reaction rate [106]. Direct measurements have been carried out in the α-particle energy range of E_α = 1.14−2.33 MeV [33]. Two resonances at 1.14 (4^+) and at 1.79 MeV (1^-) were identified. The observed interference pattern points to non-resonant reaction contributions as well. These measurements were complemented by indirect transfer studies that aimed to independently confirm the strength of the resonance contributions at lower energies. Transfer measurements also confirmed the results of the resonance states studied directly [106]. Figure 4 shows the R-matrix analysis of the ^{17}O$(n, \alpha)^{14}$C reaction that includes an extrapolation toward lower energies. The level parameters for the low-energy resonances in

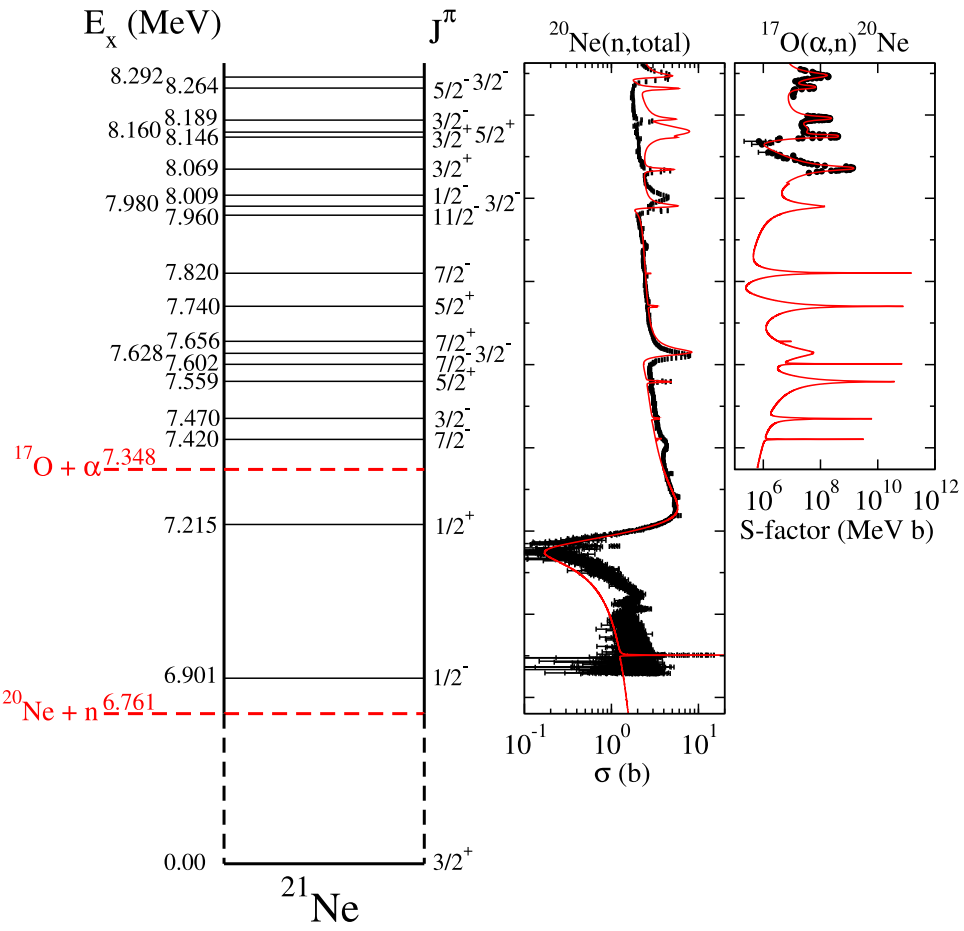

Fig. 7 Level diagram of the ^{21}Ne system near the neutron and α-particle separation energies. The levels shown are those reported in the direct measurement by Best et al. [109] over the range of their $^{17}O(\alpha, n)^{20}Ne$ data, the α-transfer study of Hammache et al. [113] between the lowest energy data of Best et al. [109] and the α-separation energy and two levels from the compilation between the α-particle and neutron separation energies. The level parameters are used to make R-matrix calculations of the cross sections for both the $^{17}O(\alpha, n)^{20}Ne$ and $^{20}Ne+n$ total cross sections and are compared to the $^{17}O(\alpha, n)^{20}Ne$ data of Best et al. [109] and the $^{nat}Ne+n$ total cross section data of Junghans et al. [115]

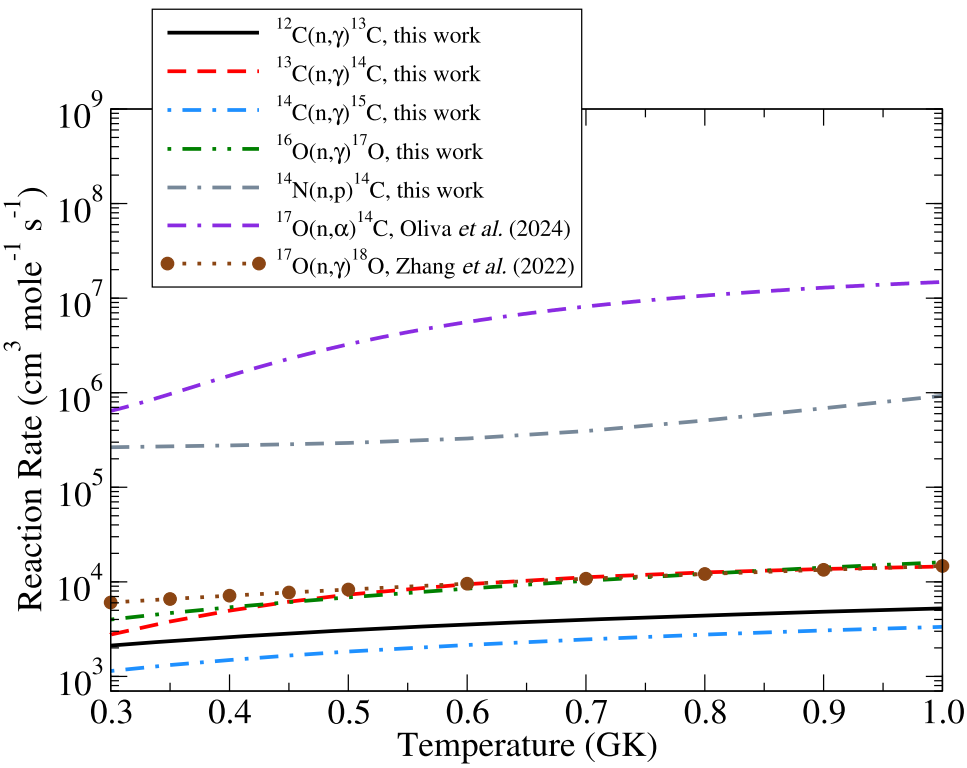

Fig. 8 Reaction rates for the $^{12,13,14}C(n, \gamma)^{13,14,15}$, $^{14}N(n, p)^{14}C$ and $^{16}O(n, \gamma)^{17}O$ reactions calculated from the R-matrix cross sections shown in Figs. 1, 2 and 6, respectively. While the rates for the $^{17}O(n, \alpha)^{14}C$ and $^{17}O(n, \gamma)^{18}O$ reactions were taken from Oliva et al. [81] and Zhang et al. [91], respectively. p-wave direct radiative capture and resonance contributions dominate the cross sections over the helium burning temperature range

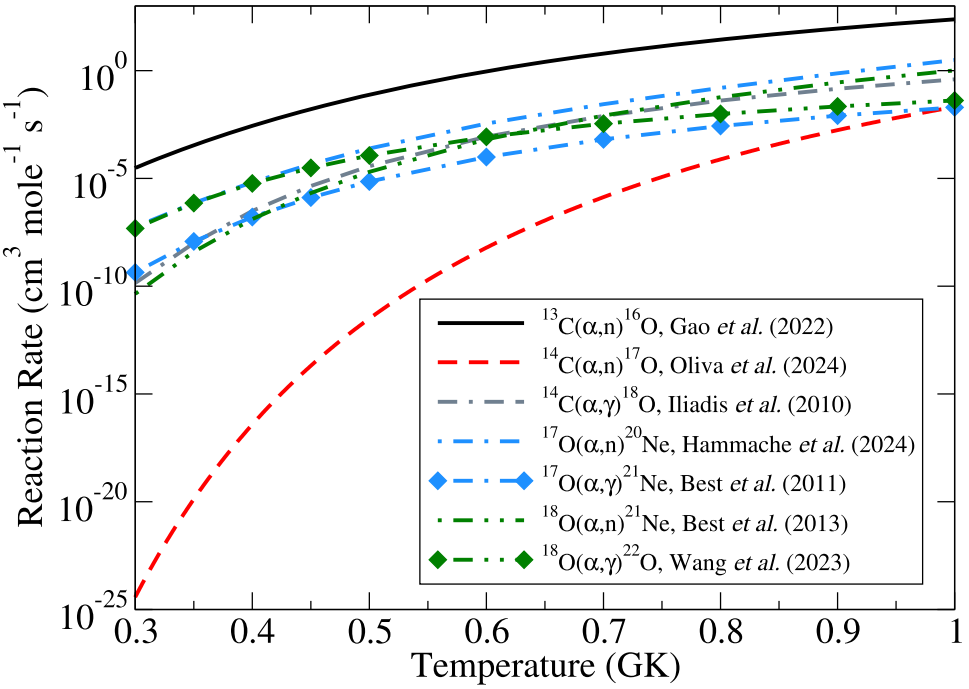

Fig. 9 The reaction rates of the $^{13}C(\alpha, n)^{16}O$ [97], $^{14}C(\alpha, n)^{17}O$ [81], $^{14}C(\alpha, \gamma)^{18}O$ [117], $^{17}O(\alpha, n)^{20}Ne$ [113], $^{17}O(\alpha, \gamma)^{21}Ne$ [116], $^{18}O(\alpha, n)^{21}Ne$ [118] and $^{18}O(\alpha, \gamma)^{22}Ne$ [119] reactions as a function of temperature over the typical range of helium burning environments

the $^{14}C(\alpha, \gamma_1)^{18}O$ transition were taken from Meltzow et al. [107], Johnson et al. [106] and the compilation [108].

Earlier studies of the $^{17}O(\alpha, n)^{20}Ne$ reaction demonstrate that the reaction cross section is characterized by a multitude of narrow resonances, which dominate the reaction rate [109]. This is supported by a recent analysis of existing $^{20}Ne(d, p)^{21}Ne$ nuclear structure data, which rely on new measurements of the neutron spectroscopic factor of low energy resonance states in the ^{21}Ne compound nucleus [110]. This study suggests strong contributions from a number of low-energy resonances. This conclusion rests on statistical assumptions sampling the reduced α-particle width from a Porter-Thomas distribution [24] normalized to more recent direct measurements of the resonance strengths [111]. This approach does not include the possibility of threshold effects, which could cause a considerable modification in the reaction rate [112]. In particular, there a $1/2^+$ state at $E_x = 7.215$ MeV that could produce a pronounced subthreshold d-wave state for α-capture on ^{17}O. Alpha transfer studies indeed suggest considerably stronger α-cluster strength for levels near the threshold leading to an enhancement in the $^{17}O(\alpha, n)^{20}Ne$ and $^{17}O(\alpha, \gamma)^{21}Ne$ reaction rates [113].

Indeed, the consistency in the α-widths between direct and transfer measurements is questionable. In Hammache et al. [113], there is only a single level that was populated by the α-transfer reaction of that work and the direct measurements of Best et al. [109] at E_x = 8069 keV. In Hammache et al. [113] the α-width was found to be 1.54(54) meV, while in Best et al. [109] it was found to be 46.2(46) meV. In addition, Mohr [114] has highlighted inconsistencies with the higher energy measurements of Best et al. [109] that influence the rate above ≈1 GK. Because of this large discrepancy, further experimental measurements are urgently needed. Figure 7 shows the present R-matrix analysis of the data based on Best et al. [109], Williams et al. [111] and Hammache et al. [113].

Figure 9 shows a comparison of the α- and neutron-induced capture processes on ^{17}O. The overall reaction rates for $^{17}O(\alpha, n)^{20}Ne$ and $^{17}O(\alpha, \gamma)^{21}Ne$, which both decline with decreasing temperature due to the Coulomb barrier are shown in Fig. 9. The rates are taken from the recent works of Hammache et al. [113] and Best et al. [116], respectively. The $^{17}O(n, \alpha)^{14}C$ and $^{17}O(n, \gamma)^{18}O$ neutron capture rates, shown in Fig. 8 and taken from Oliva et al. [81] (using time-reversal symmetry) and Zhang et al. [91], respectively, are not subject to the Coulomb barrier and are larger by several orders of magnitude than the rates for the α induced reactions. However, the mass fraction of α particles in a ^4He burning environment is considerably larger than the relative weak neutron flux.

Neutrons are produced by the $^{13}C(\alpha, n)^{16}O$ reaction at typical temperatures of ≈ 0.3 GK in helium burning environments. The next strongest neutron production process is $^{17}O(\alpha, n)^{20}Ne$, with a rate that is about two orders of magnitude smaller (see Fig. 9). Depending on the mass fraction of CNO isotopes, a balance between neutron production and neutron absorption processes will be established in this temperature range, presumably leaving a net flux of neutrons for the s-process. The additional neutron flux depends not only on the CNO abundances but also on the storage time in the nCNO cycle as will be simulated in a forthcoming paper.

6 Summary and conclusion

Light CNO isotopes are expected to be present in temperature-dependent equilibrium abundances in typical *s*-process environments, such as the end of the helium burning phase of massive stars for the weak *s*-process as well as in the carbon pocket projected for the hydrogen-helium inter-shell region feeding the main *s*-process. Neutron capture reactions on such light isotopes have been identified as neutron absorbers, typically labeled neutron poisons, but this paper seeks to argue that these neutron absorption processes are closely correlated with (α, n) reactions, often feeding the same compound nuclei. Neutron absorption therefore only causes temporary neutron storage in the respective compound systems of the here proposed nCNO cycle. The equilibrium is facilitated through the level structure of the associated oxygen compound nuclei, such as ^{17}O for ^{13}C$(\alpha, n)^{16}$O and ^{16}O$(n, \gamma)^{17}$O, ^{18}O for ^{14}C$(\alpha, \gamma)^{18}$O and ^{17}O$(n, \alpha)^{14}$C and ^{17}O$(n, \gamma)^{18}$O, as well as ^{21}Ne for ^{17}O$(\alpha, n)^{20}$Ne and ^{20}Ne$(n, \gamma)^{21}$Ne reactions, respectively. From the emerging abundance distribution in the cycles, neutrons are released through ^{13}C$(\alpha, n)^{16}$O, ^{17}O$(\alpha, n)^{20}$Ne, ^{14}C$(\alpha, \gamma)^{18}$O$(\alpha, n)^{21}$Ne, and ^{18}O$(\alpha, \gamma)^{22}$Ne$(\alpha, n)^{25}$Mg reactions at temperature conditions that are determined by the associated reaction rates. While the ^{13}C$(\alpha, n)^{16}$O reaction initiates the neutron production process, the ^{17}O$(\alpha, n)^{20}$Ne rate is significantly enhanced due to recently investigated threshold resonances and contributes at lower than expected temperatures. The ^{14}C$(\alpha, \gamma)^{18}$O reaction shifts the abundance distribution into the oxygen range from which the higher Z neutron source sequence ^{18}O$(\alpha, \gamma)^{22}$Ne$(\alpha, n)^{25}$Mg can be fueled depending on the temperature and density development in the local environment. Detailed network simulations of these intertwined cyclic processes are in preparation and will be subject to a forthcoming paper.

Acknowledgements This research utilized resources from the University of Notre Dame Center for Research Computing and was supported in part by the National Science Foundation through Grant No. PHY-2011890 (University of Notre Dame Nuclear Science Laboratory) and Grant No. OISE-1927130 (IReNA).

Data Availability Statement Data will be made available on reasonable request. [Authors' comment: The datasets generated during and/or analysed during the current study are available from the corresponding author on reasonable request.].

Code Availability Statement This manuscript has no associated code/software. [Authors' comment: Code/Software sharing not applicable to this article as no code/software was generated or analysed during the current study.].

References

1. M. Busso, R. Gallino, The production of neutron-rich isotopes during He burning in massive stars. A&A **151**, 205 (1985)
2. Z.Y. Bao, F. Käppeler, Neutron capture cross sections for *s*-process studies. At. Data Nucl. Data Tables **36**, 411 (1987). https://doi.org/10.1016/0092-640X(87)90011-8
3. H. Beer, F. Voss, R.R. Winters, On the calculation of Maxwellian-averaged capture cross sections. ApJS **80**, 403 (1992). https://doi.org/10.1086/191669
4. M. Wiescher, J. Görres, F.-K. Thielemann, Capture reactions on ^{14}C in nonstandard big bang nucleosynthesis. ApJ **363**, 340 (1990). https://doi.org/10.1086/169348
5. H. Beer, M. Wiescher, F. Käppeler, J. Görres, P.E. Koehler, A measurement of the ^{14}C$(n, \gamma)^{15}$C cross section at a Stellar temperature of kT = 23.3 keV. ApJ **387**, 258 (1992). https://doi.org/10.1086/171077
6. M. Lugaro, M. Pignatari, R. Reifarth, M. Wiescher, The *s*-process and beyond. Annu. Rev. Nucl. Part. Sci. **73**, 315 (2023). https://doi.org/10.1146/annurev-nucl-102422-080857
7. R.H. Cyburt, B.D. Fields, K.A. Olive, T.-H. Yeh, Big bang nucleosynthesis: present status. Rev. Mod. Phys. **88**, 015004 (2016). https://doi.org/10.1103/RevModPhys.88.015004. arXiv:1505.01076 [astro-ph.CO]
8. A. Coc, S. Goriely, Y. Xu, M. Saimpert, E. Vangioni, Standard big bang nucleosynthesis up to CNO with an improved extended nuclear network. ApJ **744**, 158 (2012). https://doi.org/10.1088/0004-637X/744/2/158. arXiv:1107.1117 [astro-ph.CO]
9. R.S. de Souza, S.R. Boston, A. Coc, C. Iliadis, Thermonuclear fusion rates for tritium + deuterium using Bayesian methods. Phys. Rev. C **99**, 014619 (2019). https://doi.org/10.1103/PhysRevC.99.014619. arXiv:1901.04857 [nucl-th]
10. A. Aprahamian, R. James deBoer, J. Görres, M.Q. Sorensen, M. Wiescher, M. Gatu-Johnson, C.J. Forrest, A. Schwemmlein, Nucleosynthesis with tritium. J. Phys. G Nucl. Phys. **52**, 063001 (2025). https://doi.org/10.1088/1361-6471/addc86
11. S. Bisterzo, R. Gallino, F. Käppeler, M. Wiescher, G. Imbriani, O. Straniero, S. Cristallo, J. Görres, R.J. deBoer, arXiv:1507.06798 [astro-ph.SR], The branchings of the main s-process: their sensitivity to α-induced reactions on ^{13}C and ^{22}Ne and to the uncertainties of the nuclear network. MNRAS **449**, 506 (2015). https://doi.org/10.1093/mnras/stv271
12. A. Psaltis, A. Arcones, M.L. Avila, M. Jacobi, C.J. Hansen, L. Lombardo, Z. Meisel, P. Mohr, F. Montes, W.J. Ong, H. Schatz, Constraining nucleosythesis in neutrino-driven winds using the impact of (α, xn) reaction rates. Eur. Phys. J. Web Conf. **279**, 08002 (2023). https://doi.org/10.1051/epjconf/202327908002
13. C.M. Raiteri, R. Gallino, M. Busso, D. Neuberger, F. Käppeler, The weak *s*-component and nucleosynthesis in massive stars. ApJ **419**, 207 (1993). https://doi.org/10.1086/173476
14. M. Busso, G. Picchio, R. Gallino, A. Chieffi, Are *s*-elements really produced during thermal pulses in intermediate-mass stars? ApJ **326**, 196 (1988). https://doi.org/10.1086/166081
15. F. Käppeler, R. Gallino, M. Busso, G. Picchio, C.M. Raiteri, *s*-process nucleosynthesis: classical approach and asymptotic giant

branch models for low-mass stars. ApJ **354**, 630 (1990). https://doi.org/10.1086/168720
16. R.E. Azuma, E. Uberseder, E.C. Simpson, C.R. Brune, H. Costantini, R.J. de Boer, J. Görres, M. Heil, P.J. Leblanc, C. Ugalde, M. Wiescher, AZURE: an *R*-matrix code for nuclear astrophysics. Phys. Rev. C **81**, 045805 (2010). https://doi.org/10.1103/PhysRevC.81.045805
17. J. Görres, C. Arlandini, U. Giesen, M. Heil, F. Käppeler, H. Leiste, E. Stech, M. Wiescher, Low-energy resonances in ^{14}N(α,γ)^{18}F and their astrophysical implications. Phys. Rev. C **62**, 055801 (2000). https://doi.org/10.1103/PhysRevC.62.055801
18. H.P. Trautvetter, M. Wiescher, K.U. Kettner, C. Rolfs, J.W. Hammer, Helium burning of ^{18}O. Nucl. Phys. A **297**, 489 (1978). https://doi.org/10.1016/0375-9474(78)90156-2
19. S. Dababneh, M. Heil, F. Käppeler, J. Görres, M. Wiescher, R. Reifarth, H. Leiste, Stellar He burning of ^{18}O: a measurement of low-energy resonances and their astrophysical implications. Phys. Rev. C **68**, 025801 (2003). https://doi.org/10.1103/PhysRevC.68.025801
20. A.C. Dombos, D. Robertson, A. Simon, T. Kadlecek, M. Hanhardt, J. Görres, M. Couder, R. Kelmar, O. Olivas-Gomez, E. Stech, F. Strieder, M. Wiescher, Measurement of low-energy resonance strengths in the ^{18}O (α,γ)^{22}Ne reaction. Phys. Rev. Lett. **128**, 162701 (2022). https://doi.org/10.1103/PhysRevLett.128.162701
21. H.W. Drotleff, A. Denker, J.W. Hammer, H. Knee, S. Küchler, D. Streit, C. Rolfs, H.P. Trautvetter, New ^{22}Ne(α, n)^{25}Mg-resonances at very low energies relevant for the astrophysical *s*-process. Z. Phys. A Hadrons Nucl. **338**, 367 (1991). https://doi.org/10.1007/BF01288203
22. H.W. Drotleff, A. Denker, H. Knee, M. Soine, G. Wolf, J.W. Hammer, U. Greife, C. Rolfs, H.P. Trautvetter, Reaction rates of the *s*-process neutron sources ^{22}Ne(α, *n*)^{25}Mg and ^{13}C(α, *n*)^{16}O. ApJ **414**, 735 (1993). https://doi.org/10.1086/173119
23. M. Jaeger, R. Kunz, A. Mayer, J.W. Hammer, G. Staudt, K.L. Kratz, B. Pfeiffer, ^{22}Ne(α, n)^{25}Mg: the key neutron source in massive stars. Phys. Rev. Lett. **87**, 202501 (2001). https://doi.org/10.1103/PhysRevLett.87.202501
24. R. Longland, C. Iliadis, A.I. Karakas, Reaction rates for the *s*-process neutron source ^{22}Ne + α. Phys. Rev. C **85**, 065809 (2012). https://doi.org/10.1103/PhysRevC.85.065809. arXiv:1206.3871 [astro-ph.SR]
25. M. Wiescher, R.J. deBoer, J. Görres, The resonances in the ^{22}Ne+α fusion reactions. Eur. Phys. J. A **59**, 11 (2023). https://doi.org/10.1140/epja/s10050-023-00917-9
26. P. Adsley, U. Battino, A. Best, A. Caciolli, A. Guglielmetti, G. Imbriani, H. Jayatissa, M. La Cognata, L. Lamia, E. Masha, C. Massimi, S. Palmerini, A. Tattersall, R. Hirschi, Reevaluation of the ^{22}Ne(α,γ)^{26}Mg and ^{22}Ne(α, n)^{25}Mg reaction rates. Phys. Rev. C **103**, 015805 (2021). https://doi.org/10.1103/PhysRevC.103.015805. arXiv:2005.14482 [nucl-ex]
27. Shahina, R.J. deBoer, J. Görres, R. Fang, M. Febbraro, R. Kelmar, M. Matney, K. Manukyan, J.T. Nattress, E. Robles, T.J. Ruland, T.T. King, A. Sanchez, R.S. Sidhu, E. Stech, M. Wiescher, Strength measurement of the E $^{lab}_{\alpha}$=830 keV resonance in the ^{22}Ne(α, n)^{25}Mg reaction using a stilbene detector. Phys. Rev. C **110**, 015801 (2024). https://doi.org/10.1103/PhysRevC.110.015801. arXiv:2409.01393 [nucl-ex]
28. F. Käppeler, M. Wiescher, U. Giesen, J. Görres, I. Baraffe, M. El Eid, C.M. Raiteri, M. Busso, R. Gallino, M. Limongi, A. Chieffi, Reaction rates for ^{18}O(α, γ)^{22}Ne, ^{22}Ne(α, γ)^{26}Mg, and ^{22}Ne(α, *n*)^{25}Mg in stellar helium burning and *s*-process nucleosynthesis in massive stars. ApJ **437**, 396 (1994). https://doi.org/10.1086/175004
29. M. Pignatari, R. Gallino, M. Heil, M. Wiescher, F. Käppeler, F. Herwig, S. Bisterzo, The weak s-process in massive stars and its dependence on the neutron capture cross sections. ApJ **710**, 1557 (2010). https://doi.org/10.1088/0004-637X/710/2/1557
30. M. Freer, H.O.U. Fynbo, The Hoyle state in ^{12}C. Prog. Part. Nucl. Phys. **78**, 1 (2014). https://doi.org/10.1016/j.ppnp.2014.06.001
31. R.J. deBoer, J. Görres, M. Wiescher, R.E. Azuma, A. Best, C.R. Brune, C.E. Fields, S. Jones, M. Pignatari, D. Sayre, K. Smith, F.X. Timmes, E. Uberseder, The ^{12}C(α,γ)^{16}O reaction and its implications for stellar helium burning. Rev. Mod. Phys. **89**, 035007 (2017). https://doi.org/10.1103/RevModPhys.89.035007. arXiv:1709.03144 [nucl-ex]
32. R. Reifarth, M. Heil, R. Plag, U. Besserer, S. Dababneh, L. Dörr, J. Görres, R.C. Haight, F. Käppeler, A. Mengoni, S. O'Brien, N. Patronis, R.S. Rundberg, M. Wiescher, J.B. Wilhelmy, Stellar neutron capture rates of ^{14}C. Nucl. Phys. A **758**, 787 (2005). https://doi.org/10.1016/j.nuclphysa.2005.05.141
33. J. Görres, S. Graff, M. Wiescher, R.E. Azuma, C.A. Barnes, T.R. Wang, Alpha capture on ^{14}C and its astrophysical implications. Nucl. Phys. A **548**, 414 (1992). https://doi.org/10.1016/0375-9474(92)90692-D
34. T. Kikuchi, Y. Nagai, T.S. Suzuki, T. Shima, T. Kii, M. Igashira, A. Mengoni, T. Otsuka, Nonresonant direct *p*- and *d*-wave neutron capture by ^{12}C. Phys. Rev. C **57**, 2724 (1998). https://doi.org/10.1103/PhysRevC.57.2724. arXiv:nucl-th/9802051
35. P. Mohr, C. Heinz, M. Pignatari, I. Dillmann, A. Mengoni, F. Käppeler, Re-evaluation of the ^{16}O(n, γ)^{17}O cross section at astrophysical energies and its role as a neutron poison in the s-process. ApJ **827**, 29 (2016). https://doi.org/10.3847/0004-637X/827/1/29. arXiv:1605.02639 [astro-ph.SR]
36. H. Beer, G. Rupp, F. Voss, F. Käppeler, A measurement of the ^{22}Ne(n, γ)^{23}Ne capture cross section at a stellar temperature of kT = 25 keV. ApJ **379**, 420 (1991). https://doi.org/10.1086/170518
37. C. Massimi, P. Koehler, S. Bisterzo, N. Colonna, R. Gallino, F. Gunsing, F. Käppeler, G. Lorusso, A. Mengoni, M. Pignatari, G. Vannini, U. Abbondanno, G. Aerts, H. Álvarez, F. Álvarez-Velarde, S. Andriamonje, J. Andrzejewski, P. Assimakopoulos, L. Audouin, G. Badurek, M. Barbagallo, P. Baumann, F. Bečvář, F. Belloni, M. Bennett, E. Berthoumieux, M. Calviani, F. Calviño, D. Cano-Ott, R. Capote, C. Carrapiço, A. Carrillo de Albornoz, P. Cennini, V. Chepel, E. Chiaveri, G. Cortes, A. Couture, J. Cox, M. Dahlfors, S. David, I. Dillmann, R. Dolfini, C. Domingo-Pardo, W. Dridi, I. Duran, C. Eleftheriadis, M. Embid-Segura, L. Ferrant, A. Ferrari, R. Ferreira-Marques, L. Fitzpatrick, H. Frais-Koelbl, K. Fujii, W. Furman, I. Goncalves, E. González-Romero, A. Goverdovski, F. Gramegna, E. Griesmayer, C. Guerrero, B. Haas, R. Haight, M. Heil, A. Herrera-Martinez, F. Herwig, R. Hirschi, M. Igashira, S. Isaev, E. Jericha, Y. Kadi, D. Karadimos, D. Karamanis, M. Kerveno, V. Ketlerov, V. Konovalov, S. Kopecky, E. Kossionides, M. Krtička, C. Lampoudis, H. Leeb, C. Lederer, A. Lindote, I. Lopes, R. Losito, M. Lozano, S. Lukic, J. Marganiec, L. Marques, S. Marrone, T. Martínez, P. Mastinu, E. Mendoza, P.M. Milazzo, C. Moreau, M. Mosconi, F. Neves, H. Oberhummer, S. O'Brien, M. Oshima, J. Pancin, C. Papachristodoulou, C. Papadopoulos, C. Paradela, N. Patronis, A. Pavlik, P. Pavlopoulos, L. Perrot, M.T. Pigni, R. Plag, A. Plompen, A. Plukis, A. Poch, J. Praena, C. Pretel, J. Quesada, T. Rauscher, R. Reifarth, G. Rockefeller, M. Rosetti, C. Rubbia, G. Rudolf, J. Salgado, C. Santos, L. Sarchiapone, R. Sarmento, I. Savvidis, C. Stephan, G. Tagliente, J.L. Tain, D. Tarrío, L. Tassan-Got, L. Tavora, R. Terlizzi, P. Vaz, A. Ventura, D. Villamarin, V. Vlachoudis, R. Vlastou, F. Voss, S. Walter, H. Wendler, M. Wiescher, K. Wisshak, Resonance neutron-capture cross sections of stable magnesium isotopes and their astrophysical implications. Phys. Rev. C **85**, 044615 (2012). https://doi.org/10.1103/PhysRevC.85.044615
38. C. Massimi, S. Altstadt, J. Andrzejewski, L. Audouin, M. Barbagallo, V. Bécares, F. Bečvář, F. Belloni, E. Berthoumieux, J.

Billowes, S. Bisterzo, D. Bosnar, M. Brugger, M. Calviani, F. Calviño, D. Cano-Ott, C. Carrapiço, D.M. Castelluccio, F. Cerutti, E. Chiaveri, L. Cosentino, M. Chin, G. Clai, N. Colonna, G. Cortés, M.A. Cortés-Giraldo, S. Cristallo, M. Diakaki, C. Domingo-Pardo, I. Duran, R. Dressler, C. Eleftheriadis, A. Ferrari, P. Finocchiaro, K. Fraval, S. Ganesan, A.R. García, G. Giubrone, I.F. Gonçalves, E. González-Romero, E. Griesmayer, C. Guerrero, F. Gunsing, A. Hernández-Prieto, D.G. Jenkins, E. Jericha, Y. Kadi, F. Käppeler, D. Karadimos, N. Kivel, P. Koehler, M. Kokkoris, S. Kopecky, M. Krtička, J. Kroll, C. Lampoudis, C. Langer, E. Leal-Cidoncha, C. Lederer, H. Leeb, L.S. Leong, S. Lo Meo, R. Losito, A. Mallick, A. Manousos, J. Marganiec, T. Martínez, P.F. Mastinu, M. Mastromarco, E. Mendoza, A. Mengoni, P.M. Milazzo, F. Mingrone, M. Mirea, W. Mondelaers, A. Musumarra, C. Paradela, A. Pavlik, J. Perkowski, M. Pignatari, L. Piersanti, A. Plompen, J. Praena, J.M. Quesada, T. Rauscher, R. Reifarth, A. Riego, M.S. Robles, C. Rubbia, M. Sabaté-Gilarte, R. Sarmento, A. Saxena, P. Schillebeeckx, S. Schmidt, D. Schumann, G. Tagliente, J.L. Tain, D. Tarrío, L. Tassan-Got, A. Tsinganis, S. Valenta, G. Vannini, I. Van Rijs, V. Variale, P. Vaz, A. Ventura, M.J. Vermeulen, V. Vlachoudis, R. Vlastou, A. Wallner, T. Ware, M. Weigand, C. Weiß, R. Wynants, T. Wright, P. Žugec, Neutron spectroscopy of ^{26}Mg states: Constraining the stellar neutron source ^{22}Ne(α, n)^{25}Mg. Phys. Lett. B **768**, 1 (2017). https://doi.org/10.1016/j.physletb.2017.02.025. arXiv:1702.04520 [nucl-ex]

39. Y. Chen, G.P.A. Berg, R.J. deBoer, J. Görres, H. Jung, A. Long, K. Seetedohnia, R. Talwar, M. Wiescher, S. Adachi, H. Fujita, Y. Fujita, K. Hatanaka, C. Iwamoto, B. Liu, S. Noji, H.J. Ong, A. Tamii, Neutron transfer studies on ^{25}Mg and its correlation to neutron radiative capture processes. Phys. Rev. C **103**, 035809 (2021). https://doi.org/10.1103/PhysRevC.103.035809
40. Shahina, A. Boeltzig, K. Macon, R. deBoer, M. Febbraro, S. Aguilar, T. Anderson, S. Burcher, Y. Chen, A. Clark, A. Dombos, C. Dulal, B. Frentz, G. Gilardy, O. Gomez, J. Görres, A. Gula, S. Henderson, K. Howard, J. Kovoor, K. Jones, J. Kelley, R. Kelmar, J. Kovoor, Q. Liu, A. Majumdar, K. Manukyan, L. Morales, S. Mosby, S. Moylan, A. Nelson, S. Pain, C. Reingold, M. Renaud, N. Sensharma, C. Seymour, E. Stech, W. Tan, R. Toomey, B.V. de Kolk, J. Wilkinson, M. Wiescher, Low energy measurement of the ^{25}Mg(α, n)^{28}Si reaction via neutron spectroscopy. Phys. Rev. C (2025). (**submitted for review**)
41. O. Straniero, R. Gallino, M. Busso, A. Chiefei, C.M. Raiteri, M. Limongi, M. Salaris, Radiative 13C burning in asymptotic giant branch stars and s-processing. ApJ **440**, L85 (1995). https://doi.org/10.1086/187767
42. R. Gallino, C. Arlandini, M. Busso, M. Lugaro, C. Travaglio, O. Straniero, A. Chieffi, M. Limongi, Evolution and nucleosynthesis in low-mass asymptotic giant branch stars. II. Neutron capture and the S-process. ApJ **497**, 388 (1998). https://doi.org/10.1086/305437
43. S. Bisterzo, C. Travaglio, R. Gallino, M. Wiescher, F. Käppeler, Galactic chemical evolution and solar s-process abundances: dependence on the ^{13}C-pocket structure. ApJ **787**, 10 (2014). https://doi.org/10.1088/0004-637X/787/1/10. arXiv:1403.1764 [astro-ph.SR]
44. S. Bisterzo, C. Travaglio, M. Wiescher, F. Käppeler, R. Gallino, Galactic chemical evolution: the impact of the ^{13}C-pocket structure on the s-process distribution. ApJ **835**, 97 (2017). https://doi.org/10.3847/1538-4357/835/1/97. arXiv:1701.01056 [astro-ph.SR]
45. A.I. Karakas, M. Lugaro, Stellar yields from metal-rich asymptotic giant branch models. ApJ **825**, 26 (2016). https://doi.org/10.3847/0004-637X/825/1/26. arXiv:1604.02178 [astro-ph.SR]
46. S. Cristallo, O. Straniero, R. Gallino, L. Piersanti, I. Domínguez, M.T. Lederer, Evolution, nucleosynthesis, and yields of low-mass asymptotic giant branch stars at different metallicities. ApJ **696**, 797 (2009). https://doi.org/10.1088/0004-637X/696/1/797. arXiv:0902.0243 [astro-ph.SR]
47. F. Käppeler, R. Gallino, S. Bisterzo, W. Aoki, The *s*-process: nuclear physics, stellar models, and observations. Rev. Mod. Phys. **83**, 157 (2011). https://doi.org/10.1103/RevModPhys.83.157. arXiv:1012.5218 [astro-ph.SR]
48. A.I. Karakas, J.C. Lattanzio, The Dawes review 2: nucleosynthesis and stellar yields of low- and intermediate-mass single stars. PASA **31**, e030 (2014). https://doi.org/10.1017/pasa.2014.21. arXiv:1405.0062 [astro-ph.SR]
49. G. Cescutti, R. Hirschi, N. Nishimura, J.W.D. Hartogh, T. Rauscher, A.S.J. Murphy, S. Cristallo, Uncertainties in *s*-process nucleosynthesis in low-mass stars determined from Monte Carlo variations. MNRAS **478**, 4101 (2018). https://doi.org/10.1093/mnras/sty1185. arXiv:1805.01250 [astro-ph.SR]
50. P. Torres-Sánchez, J. Praena, I. Porras, M. Sabaté-Gilarte, C. Lederer-Woods, O. Aberle, V. Alcayne, S. Amaducci, J. Andrzejewski, L. Audouin, V. Bécares, V. Babiano-Suarez, M. Bacak, M. Barbagallo, F. Bečvář, G. Bellia, E. Berthoumieux, J. Billowes, D. Bosnar, A. Brown, M. Busso, M. Caamaño, L. Caballero, F. Calviño, M. Calviani, D. Cano-Ott, A. Casanovas, F. Cerutti, Y. Chen, E. Chiaveri, N. Colonna, G. Cortés, M. Cortés-Giraldo, L. Cosentino, S. Cristallo, L.-A. Damone, M. Diakaki, M. Dietz, C. Domingo-Pardo, R. Dressler, E. Dupont, I. Durán, Z. Eleme, B. Fernández-Domínguez, A. Ferrari, F.J. Ferrer, P. Finocchiaro, V. Furman, K. Göbel, R. Garg, A. Gawlik-Ramiega, B. Geslot, S. Gilardoni, T. Glodariu, I. Gonçalves, E. González-Romero, C. Guerrero, F. Gunsing, H. Harada, S. Heinitz, J. Heyse, D. Jenkins, E. Jericha, F. Käppeler, Y. Kadi, A. Kimura, N. Kivel, M. Kokkoris, Y. Kopatch, M. Krtička, D. Kurtulgil, I. Ladarescu, H. Leeb, J. Lerendegui-Marco, S.L. Meo, S.-J. Lonsdale, D. Macina, A. Manna, T. Martínez, A. Masi, C. Massimi, P. Mastinu, M. Mastromarco, F. Matteucci, E.-A. Maugeri, A. Mazzone, E. Mendoza, A. Mengoni, V. Michalopoulou, P.M. Milazzo, F. Mingrone, A. Musumarra, A. Negret, R. Nolte, F. Ogállar, A. Oprea, N. Patronis, A. Pavlik, J. Perkowski, L. Persanti, J.-M. Quesada, D. Radeck, D. Ramos-Doval, T. Rauscher, R. Reifarth, D. Rochman, C. Rubbia, A. Saxena, P. Schillebeeckx, D. Schumann, G. Smith, N. Sosnin, A. Stamatopoulos, G. Tagliente, J. Tain, Z. Talip, A. Tarifeño-Saldivia, L. Tassan-Got, A. Tsinganis, J. Ulrich, S. Urlass, S. Valenta, G. Vannini, V. Variale, P. Vaz, A. Ventura, V. Vlachoudis, R. Vlastou, A. Wallner, P. Woods, T. Wright, P. Žugec, n TOF Collaboration, Measurement of the ^{14}N(n, p)^{14}C cross section at the CERN n_TOF facility from subthermal energy to 800 keV. Phys. Rev. C **107**, 064617 (2023). https://doi.org/10.1103/PhysRevC.107.064617. arXiv:2212.05128 [nucl-ex]
51. M. Wiescher, F. Käppeler, K. Langanke, Critical reactions in contemporary nuclear astrophysics. ARA&A **50**, 165 (2012). https://doi.org/10.1146/annurev-astro-081811-125543
52. S. Dubovichenko, A. Dzhazairov-Kakhramanov, N. Afanasyeva, Radiative neutron capture on ^{9}Be, ^{14}C, ^{14}N, ^{15}N and ^{16}O at thermal and astrophysical energies. Int. J. Mod. Phys. E **22**, 1350075–60 (2013). https://doi.org/10.1142/S0218301313500754. arXiv:1312.5865 [nucl-th]
53. M. He, S.-S. Zhang, M. Kusakabe, S. Xu, T. Kajino, Nuclear structures of ^{17}O and time-dependent sensitivity of the weak s-process to the ^{16}O(n,γ)^{17}O rate. ApJ **899**, 133 (2020). https://doi.org/10.3847/1538-4357/aba7b4
54. H. Schatz, F. Käppeler, P.E. Koehler, M. Wiescher, H.P. Trautvetter, ^{17}O(n, α)^{14}C: closure of a primordial CNO bi-cycle? ApJ **413**, 750 (1993). https://doi.org/10.1086/173042
55. Y. Nagai, M. Igashira, K. Takeda, N. Mukai, S. Motoyama, F. Uesawa, H. Kitazawa, T. Fukuda, Measurement of the neutron capture rate of the ^{12}C(n, γ)^{13}C reaction at stellar energy. ApJ **372**, 683 (1991). https://doi.org/10.1086/170010

56. T. Ohsaki, Y. Nagai, M. Igashira, T. Shima, K. Takeda, S. Seino, T. Irie, New measurement of the $^{12}C(n,\gamma)^{13}C$ reaction cross section. ApJ **422**, 912 (1994). https://doi.org/10.1086/173783
57. R.B. Firestone, Z. Revay, Thermal neutron radiative cross sections for ^{6,7}Li, ^{9}Be, ^{10,11}B, ^{12,13}C and ^{14,15}N. Phys. Rev. C **93**, 054306 (2016). https://doi.org/10.1103/PhysRevC.93.054306
58. T. Shima, F. Okazaki, T. Kikuchi, T. Kobayashi, T. Kii, T. Baba, Y. Nagai, M. Igashira, Measurement of the $^{13}C(n,\gamma)^{14}C$ cross section at stellar energies. Nucl. Phys. A **621**, 231 (1997). https://doi.org/10.1016/S0375-9474(97)00243-1
59. A. Wallner, M. Bichler, K. Buczak, I. Dillmann, F. Käppeler, A. Karakas, C. Lederer, M. Lugaro, K. Mair, A. Mengoni, G. Schätzel, P. Steier, H.P. Trautvetter, Accelerator mass spectrometry measurements of the $^{13}C(n,\gamma)^{14}C$ and $^{14}N(n,p)^{14}C$ cross sections. Phys. Rev. C **93**, 045803 (2016). https://doi.org/10.1103/PhysRevC.93.045803
60. R. Reifarth, M. Heil, C. Forssén, U. Besserer, A. Couture, S. Dababneh, L. Dörr, J. Görres, R.C. Haight, F. Käppeler, A. Mengoni, S. O'Brien, N. Patronis, R. Plag, R.S. Rundberg, M. Wiescher, J.B. Wilhelmy, The $^{14}C(n,\gamma)$ cross section between 10 keV and 1 MeV. Phys. Rev. C **77**, 015804 (2008). https://doi.org/10.1103/PhysRevC.77.015804. arXiv:0910.0106 [astro-ph.IM]
61. S.F. Mughabghab, M.A. Lone, B.C. Robertson, Quantitative test of the Lane-Lynn theory of direct radiative capture of thermal neutrons by ^{12}C and ^{13}C. Phys. Rev. C **26**, 2698 (1982). https://doi.org/10.1103/PhysRevC.26.2698
62. J. Kelley, C. Sheu, J. Purcell, Energy levels of light nuclei $A = 13$. Nucl. Data Sheets **198**, 1 (2024). https://doi.org/10.1016/j.nds.2024.11.001
63. Z.H. Liu, C.J. Lin, H.Q. Zhang, Z.C. Li, J.S. Zhang, Y.W. Wu, F. Yang, M. Ruan, J.C. Liu, S.Y. Li, Z.H. Peng, Asymptotic normalization coefficients and neutron halo of the excited states in ^{12}B and ^{13}C. Phys. Rev. C **64**, 034312 (2001). https://doi.org/10.1103/PhysRevC.64.034312
64. G.F. Auchampaugh, S. Plattard, N.W. Hill, Neutron total cross-section measurements of ^{9}Be, ^{10,11}B, and ^{12,13}C from 1.0 to 14 MeV using the $^{9}Be(d,n)^{10}B$ reaction as a "White" neutron source. Nucl. Sci. Eng. **69**, 30 (1979). https://doi.org/10.13182/NSE79-A21282
65. G.M. Hale, M.W. Paris, Neutron cross sections for carbon and oxygen from new R-matrix analyses of the ^{13,14}C and ^{17}O systems. Eur. Phys. J. Web Conf. **146**, 02027 (2017). https://doi.org/10.1051/epjconf/201714602027
66. B.J. Allen, R.L. Macklin, Neutron capture cross sections of ^{13}C and ^{16}O. Phys. Rev. C **3**, 1737 (1971). https://doi.org/10.1103/PhysRevC.3.1737
67. S. Raman, M. Igashira, Y. Dozono, H. Kitazawa, M. Mizumoto, J.E. Lynn, Valence capture mechanism in resonance neutron capture by ^{13}C. Phys. Rev. C **41**, 458 (1990). https://doi.org/10.1103/PhysRevC.41.458
68. S.B. Dubovichenko, n+^{13}C capture reaction rate. Russ. Phys. J. **65**, 208 (2022). https://doi.org/10.1007/s11182-022-02624-2
69. K. Brehm, H.W. Becker, C. Rolfs, H.P. Trautvetter, F. Kappeler, W. Ratynski, The cross section of $^{14}N(n,p)^{14}C$ at stellar energies and its role as a neutron poison for S-process nucleosynthesis. Zeitschrift fur Physik A Hadrons Nuclei **330**, 167 (1988). https://doi.org/10.1007/BF01293392
70. G.A. Bartholomew, F. Brown, H.E. Gove, A.E. Litherland, E.B. Paul, Capture radiation and neutrons from the bombardment of C^{14} with protons. Can. J. Phys. **33**, 441 (1955). https://doi.org/10.1139/p55-053
71. R.M. Sanders, Study of the $C^{14}(p,n)N^{14}$ and $C^{14}(\alpha,n)O^{17}$ reactions. Phys. Rev. **104**, 1434 (1956). https://doi.org/10.1103/PhysRev.104.1434
72. J.H. Gibbons, R.L. Macklin, Total neutron yields from light elements under proton and alpha bombardment. Phys. Rev. **114**, 571 (1959). https://doi.org/10.1103/PhysRev.114.571
73. J. Görres, S. Graff, M. Wiescher, R.E. Azuma, C.A. Barnes, H.W. Becker, T.R. Wang, Proton capture on ^{14}C and its astrophysical implications. Nucl. Phys. A **517**, 329 (1990). https://doi.org/10.1016/0375-9474(90)90038-N
74. W.R. Harris, J.C. Armstrong, Elastic scattering of 1- to 2.7-MeV protons by C^{14}. Phys. Rev. **171**, 1230 (1968). https://doi.org/10.1103/PhysRev.171.1230
75. P.E. Koehler, H.A. O'Brien, $^{14}N(n,p)^{14}C$ cross section from 61 meV to 34.6 keV and its astrophysical implications. Phys. Rev. C **39**, 1655 (1989). https://doi.org/10.1103/PhysRevC.39.1655
76. T.C. Borgwardt, R.J. deBoer, A. Boeltzig, M. Couder, J. Görres, A. Gula, M. Hanhardt, K.V. Manukyan, T. Kadlecek, D. Robertson, F. Strieder, M. Wiescher, Deep underground measurement of $^{11}B(\alpha,n)^{14}N$. Phys. Rev. C **108**, 035809 (2023). https://doi.org/10.1103/PhysRevC.108.035809
77. R.J. deBoer, A.R. Junghans, R. Arquette, D. Bemmerer, A. Best, R. Beyer, A. Boeltzig, G. Clarke, J. Görres, T. Hensel, M. Matney, S.E. Müller, D. Rapagnani, A. Roberts, K. Römer, S. Turkat, K. Schmidt, J. Skowronski, A. Wagner, M. Wiescher, A. Yadav, Total cross section of $^{14}N+n$ from 01 to 12 MeV. Phys. Rev. C **112**, 025805 (2025). https://doi.org/10.1103/frgb-j5c3. arXiv:2505.04995 [nucl-ex]
78. J. Meissner, H. Schatz, H. Herndl, M. Wiescher, H. Beer, F. Käppeler, Neutron capture cross section of ^{15}N at stellar energies. Phys. Rev. C **53**, 977 (1996). https://doi.org/10.1103/PhysRevC.53.977
79. M. Wiescher, J. Görres, H. Schatz, Topical review: break-out reactions from the CNO cycles. J. Phys. G Nucl. Phys. **25**, R133 (1999). https://doi.org/10.1088/0954-3899/25/6/201
80. G.L. Guardo, L. Lamia, J.P. Fernández-García, S. Piskor, M. La Cognata, G. D'Agata, S. Palmerini, D. Vescovi, V. Burjan, R.J. deBoer, V. Kroha, D. Lattuada, J. Mrazek, A.A. Oliva, R.G. Pizzone, G.G. Rapisarda, S. Romano, M.L. Sergi, R. Spartá, A. Tumino, Asymptotic normalization coefficient investigation of the $^{17}O(d,p)$ transfer for astrophysical application to the $^{17}O(n,\alpha)^{14}C$ reaction at low energies. ApJ **975**, 32 (2024). https://doi.org/10.3847/1538-4357/ad7604
81. A.A. Oliva, R.J. deBoer, G.L. Guardo, M. La Cognata, L. Lamia, Absolute cross section of the $^{17}O(n,\alpha)^{14}C$ reaction. Phys. Rev. C **110**, 045812 (2024). https://doi.org/10.1103/PhysRevC.110.045812
82. J.K. Bair, J.L. Ford, C.M. Jones, Total neutron yield from the reaction $^{14}C(\alpha,n)^{17}O$. Phys. Rev. **144**, 799 (1966). https://doi.org/10.1103/PhysRev.144.799
83. G.L. Morgan, D.R. Tilley, G.E. Mitchell, R.A. Hilko, N.R. Roberson, Study of ^{18}O through $^{14}C+\alpha$ reactions. Nucl. Phys. A **148**, 480 (1970). https://doi.org/10.1016/0375-9474(70)90641-X
84. J.A. Weinman, E.A. Silverstein, Elastic scattering of alpha particles by Carbon-14. Phys. Rev. **111**, 277 (1958). https://doi.org/10.1103/PhysRev.111.277
85. M.L. Avila, G.V. Rogachev, V.Z. Goldberg, E.D. Johnson, K.W. Kemper, Y.M. Tchuvil'sky, A.S. Volya, α-cluster structure of ^{18}O. Phys. Rev. C **90**, 024327 (2014). https://doi.org/10.1103/PhysRevC.90.024327. arXiv:1406.6734 [nucl-ex]
86. L. Buchmann, J. D'Auria, M. Dombsky, U. Giesen, K.P. Jackson, P. McNeely, J. Powell, A. Volya, β-delayed α emission of ^{18}N: broad $J^{\pi}=1^{-}$ states in the $^{14}C + \alpha$ system. Phys. Rev. C **75**, 012804 (2007). https://doi.org/10.1103/PhysRevC.75.012804
87. J. Wagemans, C. Wagemans, R. Bieber, P. Geltenbort, Determination of the thermal neutron induced $^{17}O(n,\alpha)^{14}C$ reaction cross section. Phys. Rev. C **58**, 2840 (1998). https://doi.org/10.1103/PhysRevC.58.2840

88. K. Hida, S. Iijima, Evaluation of $^{17}O(n,\alpha)^{14}C$ cross section. J. Nucl. Sci. Technol. **28**, 447 (1991). https://doi.org/10.1080/18811248.1991.9731380
89. V.V. Ketlerov, A.A. Goverdovski, V.A. Khryachkov, V.F. Mitrofanov, Y.B. Ostapenko, R.C. Haight, P.E. Koehler, S.M. Grimes, R.S. Smith, Detailed study of double-differential cross-sections for the $^{17}O(n,\alpha)^{14}C$ reaction. Nucl. Phys. A **621**, 243 (1997). https://doi.org/10.1016/S0375-9474(97)00246-7
90. R.B. Firestone, Z. Revay, Thermal neutron capture cross sections for $^{16,171,18}O$ and ^{2}H. Phys. Rev. C **93**, 044311 (2016). https://doi.org/10.1103/PhysRevC.93.044311
91. L.-Y. Zhang, J.-J. He, M. Kusakabe, Z.-Y. He, T. Kajino, Thermonuclear $^{17}O(n,\gamma)^{18}O$ reaction rate and its astrophysical implications. ApJ **927**, 92 (2022). https://doi.org/10.3847/1538-4357/ac4697. arXiv:2110.02447 [nucl-th]
92. J. Meissner, H. Schatz, J. Görres, H. Herndl, M. Wiescher, H. Beer, F. Käppeler, Neutron capture cross section of ^{18}O and its astrophysical implications. Phys. Rev. C **53**, 459 (1996). https://doi.org/10.1103/PhysRevC.53.459
93. E. Uberseder, M. Heil, F. Käppeler, J. Görres, M. Wiescher, New measurements of the $^{19}F(n,\gamma)^{20}F$ cross section and their implications for the stellar reaction rate. Phys. Rev. C **75**, 035801 (2007). https://doi.org/10.1103/PhysRevC.75.035801
94. M. Heil, R. Plag, E. Uberseder, R. Gallino, S. Bisterzo, A. Jusevicute, F. Käppeler, C. Lederer, A. Mengoni, M. Pignatari, Stellar neutron capture cross sections of $^{20,21,22}Ne$. Phys. Rev. C **90**, 045804 (2014). https://doi.org/10.1103/PhysRevC.90.045804
95. E. Uberseder, M. Heil, F. Käppeler, C. Lederer, A. Mengoni, S. Bisterzo, M. Pignatari, M. Wiescher, Stellar (n,γ) cross sections of ^{23}Na. Phys. Rev. C **95**, 025803 (2017). https://doi.org/10.1103/PhysRevC.95.025803. arXiv:1702.01541 [nucl-ex]
96. G.F. Ciani, L. Csedreki, D. Rapagnani, M. Aliotta, J. Balibrea-Correa, F. Barile, D. Bemmerer, A. Best, A. Boeltzig, C. Broggini, C.G. Bruno, A. Caciolli, F. Cavanna, T. Chillery, P. Colombetti, P. Corvisiero, S. Cristallo, T. Davinson, R. Depalo, A. Di Leva, Z. Elekes, F. Ferraro, E. Fiore, A. Formicola, Z. Fülöp, G. Gervino, A. Guglielmetti, C. Gustavino, G. Gyürky, G. Imbriani, M. Junker, M. Lugaro, P. Marigo, E. Masha, R. Menegazzo, V. Mossa, F.R. Pantaleo, V. Paticchio, R. Perrino, D. Piatti, P. Prati, L. Schiavulli, K. Stöckel, O. Straniero, T. Szücs, M.P. Takács, F. Terrasi, D. Vescovi, S. Zavatarelli, L.U.N.A. Collaboration, Direct measurement of the $^{13}C(\alpha,n)^{16}O$ cross section into the *s*-process Gamow peak. Phys. Rev. Lett. **127**, 152701 (2021). https://doi.org/10.1103/PhysRevLett.127.152701. arXiv:2110.00303 [nucl-ex]
97. B. Gao, T.Y. Jiao, Y.T. Li, H. Chen, W.P. Lin, Z. An, L.H. Ru, Z.C. Zhang, X.D. Tang, X.Y. Wang, N.T. Zhang, X. Fang, D.H. Xie, Y.H. Fan, L. Ma, X. Zhang, F. Bai, P. Wang, Y.X. Fan, G. Liu, H.X. Huang, Q. Wu, Y.B. Zhu, J.L. Chai, J.Q. Li, L.T. Sun, S. Wang, J.W. Cai, Y.Z. Li, J. Su, H. Zhang, Z.H. Li, Y.J. Li, E.T. Li, C. Chen, Y.P. Shen, G. Lian, B. Guo, X.Y. Li, L.Y. Zhang, J.J. He, Y.D. Sheng, Y.J. Chen, L.H. Wang, L. Zhang, F.Q. Cao, W. Nan, W.K. Nan, G.X. Li, N. Song, B.Q. Cui, L.H. Chen, R.G. Ma, Z.C. Zhang, S.Q. Yan, J.H. Liao, Y.B. Wang, S. Zeng, D. Nan, Q.W. Fan, N.C. Qi, W.L. Sun, X.Y. Guo, P. Zhang, Y.H. Chen, Y. Zhou, J.F. Zhou, J.R. He, C.S. Shang, M.C. Li, S. Kubono, W.P. Liu, R.J. deBoer, M. Wiescher, M. Pignatari, JUNA Collaboration, Deep underground laboratory measurement of $^{13}C(\alpha,n)^{16}O$ in the Gamow windows of the *s* and *i*-processes. Phys. Rev. Lett **129**, 132701. https://doi.org/10.1103/PhysRevLett.129.132701. arXiv:2210.03222 [nucl-ex]
98. R.J. deBoer, M. Febbraro, D.W. Bardayan, C. Boomershine, K. Brandenburg, C. Brune, S. Coil, M. Couder, J. Derkin, S. Dede, R. Fang, A. Fritsch, A. Gula, G. Gyürky, B. Hackett, G. Hamad, Y. Jones-Alberty, R. Kelmar, K. Manukyan, M. Matney, J. McDonaugh, Z. Meisel, S. Moylan, J. Nattress, D. Odell, P. O'Malley, M.W. Paris, D. Robertson, Shahina, N. Singh, K. Smith, M.S. Smith, E. Stech, W. Tan, M. Wiescher, Measurement of the $^{13}C(\alpha,n_0)^{16}O$ differential cross section from 0.8 to 6.5 MeV. Phys. Rev. Lett. **132**, 062702 (2024). https://doi.org/10.1103/PhysRevLett.132.062702
99. M. Igashira, H. Kitazawa, K. Takaura, Valence-neutron capture in the 434 keV $p_{\frac{3}{2}}$-wave resonance of ^{16}O. Nucl. Phys. A **536**, 285 (1992). https://doi.org/10.1016/0375-9474(92)90382-T
100. M. Igashira, Y. Nagai, K. Masuda, T. Ohsaki, H. Kitazawa, Measurement of the $^{16}O(n,\gamma)^{17}O$ reaction cross section at stellar energy and the critical role of nonresonant *p*-wave neutron capture. ApJ **441**, L89 (1995). https://doi.org/10.1086/187797
101. Y. Nagai, M. Kinoshita, M. Igashira, Y. Nobuhara, H. Makii, K. Mishima, T. Shima, A. Mengoni, Nonresonant *p*-wave direct capture and interference effect observed in the $^{16}O(n,\gamma)^{17}O$ reaction. Phys. Rev. C **102**, 044616 (2020). https://doi.org/10.1103/PhysRevC.102.044616
102. R.J. Holt, H.E. Jackson, R.M. Laszewski, J.E. Monahan, J.R. Specht, Effects of channel and potential radiative transitions in the $^{17}O(\gamma,n_0)^{16}O$ reaction. Phys. Rev. C **18**, 1962 (1978). https://doi.org/10.1103/PhysRevC.18.1962
103. J.L. Fowler, C.H. Johnson, R.M. Feezel, Level structure of ^{17}O from neutron total cross sections. Phys. Rev. C **8**, 545 (1973). https://doi.org/10.1103/PhysRevC.8.545
104. S. Cierjacks, F. Hinterberger, G. Schmalz, D. Erbe, P.V. Rossen, B. Leugers, High precision time-of-flight measurements of neutron resonance energies in carbon and oxygen between 3 and 30 MeV. Nucl. Instrum. Methods **169**, 185 (1980). https://doi.org/10.1016/0029-554X(80)90119-6
105. J.K. Bair, F.X. Haas, Total neutron yield from the reactions $^{13}C(\alpha,n)^{16}O$ and $^{17,18}O(\alpha,n)^{20,21}Ne$. Phys. Rev. C **7**, 1356 (1973). https://doi.org/10.1103/PhysRevC.7.1356
106. E.D. Johnson, G.V. Rogachev, J. Mitchell, L. Miller, K.W. Kemper, $^{14}C(\alpha,\gamma)$ reaction rate. Phys. Rev. C **80**, 045805 (2009). https://doi.org/10.1103/PhysRevC.80.045805. arXiv:0910.0498 [nucl-ex]
107. B. Meltzow, E.K. Warburton, C. Ender, J. Gerl, D. Habs, U. Lauff, J. Schirmer, D. Schwalm, P. Thirolf, Measurement and significance of Γ_γ/Γ for the 7117-keV 4^+ level of ^{18}O. Phys. Rev. C **49**, 743 (1994). https://doi.org/10.1103/PhysRevC.49.743
108. D.R. Tilley, H.R. Weller, C.M. Cheves, R.M. Chasteler, Energy levels of light nuclei A = 18–19. Nucl. Phys. A **595**, 1 (1995). https://doi.org/10.1016/0375-9474(95)00338-1
109. A. Best, M. Beard, J. Görres, M. Couder, R. deBoer, S. Falahat, R.T. Güray, A. Kontos, K.L. Kratz, P.J. LeBlanc, Q. Li, S. O'Brien, N. Özkan, M. Pignatari, K. Sonnabend, R. Talwar, W. Tan, E. Uberseder, M. Wiescher, Measurement of the reaction $^{17}O(\alpha,n)^{20}Ne$ and its impact on the *s*-process in massive stars. Phys. Rev. C **87**, 045805 (2013). https://doi.org/10.1103/PhysRevC.87.045805. arXiv:1304.6443 [nucl-ex]
110. J. Frost-Schenk, P. Adsley, A.M. Laird, R. Longland, C. Angus, C. Barton, A. Choplin, C.A. Diget, R. Hirschi, C. Marshall, F. Portillo Chaves, K. Setoodehnia, The impact of $^{17}O + \alpha$ reaction rate uncertainties on the s-process in rotating massive stars. MNRAS **514**, 2650 (2022). https://doi.org/10.1093/mnras/stac1373. arXiv:2206.04167 [nucl-ex]
111. M. Williams, A.M. Laird, A. Choplin, P. Adsley, B. Davids, U. Greife, K. Hudson, D. Hutcheon, A. Lennarz, C. Ruiz, Constraints on key $^{17}O(\alpha,\gamma)^{21}Ne$ resonances and impact on the weak s process. Phys. Rev. C **105**, 065805 (2022). https://doi.org/10.1103/PhysRevC.105.065805. arXiv:2206.06016 [nucl-ex]
112. M. Wiescher, C.A. Bertulani, C.R. Brune, R.J. deBoer, A. Diaz-Torres, L.R. Gasques, K. Langanke, P. Navrátil, W. Nazarewicz, J. Okołowicz, D.R. Phillips, M. Płoszajczak, S. Quaglioni, A.

Tumino, Quantum physics of stars. Rev. Mod. Phys. **97**, 025003 (2025). https://doi.org/10.1103/RevModPhys.97.025003
113. F. Hammache, P. Adsley, L. Lamia, D.S. Harrouz, N. de Séréville, B. Bastin, A. Choplin, T. Faestermann, C. Fougères, R. Hertenberger, R. Hirschi, M. La Cognata, A. Meyer, S. Palmerini, R.G. Pizzone, F. de Oliveira Santos, S. Romano, A. Tumino, H.F. Wirth, Experimental determination of α Widths of ^{21}Ne levels in the region of astrophysical interest: new ^{17}O +α reaction rates and impact on the weak s process. Phys. Rev. Lett. **132**, 182701 (2024). https://doi.org/10.1103/PhysRevLett.132.182701
114. P. Mohr, Uncertainty of the astrophysical ^{17,18}O$(\alpha, n)^{20,21}$Ne reaction rates and the applicability of the statistical model for nuclei with A $\lesssim$20. Phys. Rev. C **96**, 045808 (2017). https://doi.org/10.1103/PhysRevC.96.045808. arXiv:1710.01002 [nucl-th]
115. A. Junghans, R. Beyer, J. Claußner, T. Kögler, S. Urlass, D. Bemmerer, A. Ferrari, R. Schwengner, A. Wagner, M. Dietz, A. Frotscher, M. Grieger, T. Hensel, M. Koppitz, F. Ludwig, S. Turkat, R. Nolte, E. Pirovano, S. Kopecky, M. Nyman, A. Plompen, P. Schillebeeckx, E. Borris, R. Reifarth, D. Veltum, M. Weigand, J. Glorius, J. Görres, U. Oberlack, D. Wenz, Neutron transmission measurements at nELBE. Eur. Phys. J. Web Conf. **239**, 01006 (2020). https://doi.org/10.1051/epjconf/202023901006
116. A. Best, J. Görres, M. Couder, R. Deboer, S. Falahat, A. Kontos, P.J. Leblanc, Q. Li, S. O'Brien, K. Sonnabend, R. Talwar, E. Uberseder, M. Wiescher, First direct measurement of resonance strengths in ^{17}O$(\alpha,\gamma)^{21}$Ne. Phys. Rev. C **83**, 052802 (2011). https://doi.org/10.1103/PhysRevC.83.052802. arXiv:1105.3096 [nucl-ex]
117. C. Iliadis, R. Longland, A.E. Champagne, A. Coc, R. Fitzgerald, Charged-particle thermonuclear reaction rates: II. Tables and graphs of reaction rates and probability density functions. Nucl. Phys. A **841**, 31 (2010). https://doi.org/10.1016/j.nuclphysa.2010.04.009. arXiv:1004.4517 [astro-ph.SR]
118. A. Best, S. Falahat, J. Görres, M. Couder, R. deBoer, R.T. Güray, A. Kontos, K.L. Kratz, P.J. LeBlanc, Q. Li, S. O'Brien, N. Özkan, K. Sonnabend, R. Talwar, E. Uberseder, M. Wiescher, Measurement of the reaction ^{18}O$(\alpha, n)^{21}$Ne. Phys. Rev. C **87**, 045806 (2013). https://doi.org/10.1103/PhysRevC.87.045806
119. L.H. Wang, J. Su, Y.P. Shen, J.J. He, M. Lugaro, B. Szányi, A.I. Karakas, L.Y. Zhang, X.Y. Li, B. Guo, G. Lian, Z.H. Li, Y.B. Wang, L.H. Chen, B.Q. Cui, X.D. Tang, B.S. Gao, Q. Wu, L.T. Sun, S. Wang, Y.D. Sheng, Y.J. Chen, H. Zhang, Z.M. Li, L.Y. Song, X.Z. Jiang, W. Nan, W.K. Nan, L. Zhang, F.Q. Cao, T.Y. Jiao, L.H. Ru, J.P. Cheng, M. Wiescher, W.P. Liu, Measurement of the ^{18}O$(\alpha,\gamma)^{22}$Ne reaction rate at JUNA and its impact on probing the origin of SiC grains. Phys. Rev. Lett. **130**, 092701 (2023). https://doi.org/10.1103/PhysRevLett.130.092701